Cell Metabolism

Article

Complementary lateral hypothalamic populations resist hunger pressure to balance nutritional and social needs

Graphical abstract

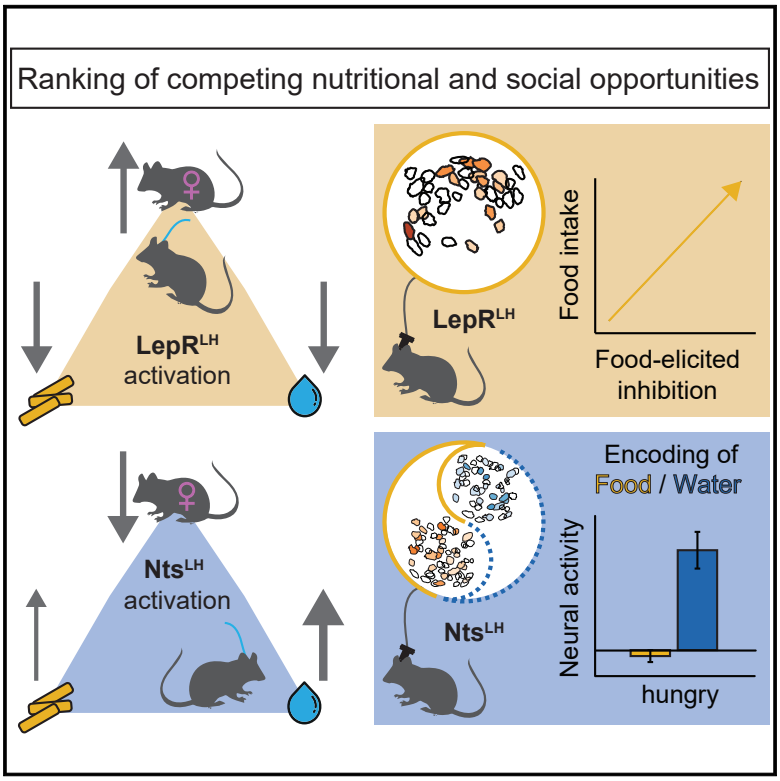

Highlights

- Food-elicited inhibition of LepR^{LH} neurons facilitates food intake
- Activation of LepR^{LH} cells limits feeding rebound post-acute food restriction
- LepR^{LH} neurons limit nutritional needs in favor of sex-specific social interaction
- Nts^{LH} neurons relegate hunger and social interaction to promote drinking

Authors

Anne Petzold,
Hanna Elin van den Munkhof,
Rebecca Figge-Schlensok,
Tatiana Korotkova

Correspondence

tatiana.korotkova@uk-koeln.de

In brief

Animals continuously weigh hunger and thirst against competing needs, such as social contact and mating, according to state and opportunity. Here, Petzold et al. show that leptin receptor-expressing and neurotensin-expressing neurons in the lateral hypothalamus resist immediate nutritional needs and flexibly prioritize competing needs despite hunger or thirst.

Petzold et al., 2023, Cell Metabolism *35*, 1–16
March 7, 2023
https://doi.org/10.1016/j.cmet.2023.02.008

CellPress

Cell Metabolism

CellPress
OPEN ACCESS

Article

Complementary lateral hypothalamic populations resist hunger pressure to balance nutritional and social needs

Anne Petzold,[1,2] Hanna Elin van den Munkhof,[1,2] Rebecca Figge-Schlensok,[1,2] and Tatiana Korotkova[1,2,3,4,*]
[1]Institute for Systems Physiology, Faculty of Medicine, University of Cologne and University Clinic Cologne, Cologne 50931, Germany
[2]Max Planck Institute for Metabolism Research, Cologne 50931, Germany
[3]Excellence Cluster on Cellular Stress Responses in Aging Associated Diseases (CECAD) and Center of Molecular Medicine Cologne (CMMC), University of Cologne, Cologne 50931, Germany
[4]Lead contact
*Correspondence: tatiana.korotkova@uk-koeln.de
https://doi.org/10.1016/j.cmet.2023.02.008

SUMMARY

Animals continuously weigh hunger and thirst against competing needs, such as social contact and mating, according to state and opportunity. Yet neuronal mechanisms of sensing and ranking nutritional needs remain poorly understood. Here, combining calcium imaging in freely behaving mice, optogenetics, and chemogenetics, we show that two neuronal populations of the lateral hypothalamus (LH) guide increasingly hungry animals through behavioral choices between nutritional and social rewards. While increased food consumption was marked by increasing inhibition of a leptin receptor-expressing ($LepR^{LH}$) subpopulation at a fast timescale, $LepR^{LH}$ neurons limited feeding or drinking and promoted social interaction despite hunger or thirst. Conversely, neurotensin-expressing LH neurons preferentially encoded water despite hunger pressure and promoted water seeking, while relegating social needs. Thus, hunger and thirst gate both LH populations in a complementary manner to enable the flexible fulfillment of multiple essential needs.

INTRODUCTION

Obesity, one of the leading causes of preventable death in the world, is characterized by an inability to resist hunger, which leads to overeating and obesity along with associated detrimental health disorders. A healthy animal adapts the motivation to engage with food, water, or conspecifics to the current physiological state through homeostatic regulation. Physiological states are monitored by neurochemically defined hypothalamic populations that encode consumptive stimuli in a need-based manner to facilitate feeding,[1–5] drinking,[6,7] and mating.[8–10] Importantly, motivational drives compete with each other. For instance, as long as energy levels are not critically low, an animal must be able to temporarily resist hunger even against homeostatic pressure to satisfy other crucial, connected needs such as balancing food and water intake[11,12] as well as to meet competing needs such as the pursuit of mating opportunities.[13,14]

The lateral hypothalamus (LH) drives food and water intake through multiple heterogeneous neuronal populations.[15–17] It remains elusive whether LH populations are gated by hunger or thirst, encode nutritional rewards alongside with social rewards, or integrate social drives with nutritional needs. Several GABAergic subpopulations of the LH regulate appetitive or food- or water-rewarded behaviors.[15–20] Among them, a subpopulation that expresses the leptin receptor—$LepR^{LH}$ neurons—enhances food-rewarded behaviors[21–24] and affects food intake depending on the state of the animal as well as the availability and palatability of food,[22,24–26] indicating that the contribution of the $LepR^{LH}$ population to the pursuit of nutritional rewards changes with state and opportunity. It is unknown whether $LepR^{LH}$ neurons rank multiple needs, such as food and water, and whether the physiological state gates the integration and ranking of multiple needs via the $LepR^{LH}$ population.

$LepR^{LH}$ neurons partially overlap with another GABAergic LH subpopulation—neurotensin-expressing LH (Nts^{LH}) neurons, which are sensitive to thirst.[27] While the activation of Nts^{LH} neurons consistently facilitates the pursuit of water independent of deprivation state,[28,29] Nts^{LH}-mediated effects on food intake are state- and time-dependent.[28–31] This suggests that hunger may differentially gate the encoding of food and water by Nts^{LH} neurons and their contribution to feeding or drinking.

Here, we investigated whether $LepR^{LH}$ and Nts^{LH} populations are capable of encoding nutritional as well as non-nutritional stimuli such as conspecifics, and whether they integrate the need for social contact, food, and water with hunger or thirst to determine the hierarchy between these competing needs.

We performed deep-brain Ca^{2+} imaging of $LepR^{LH}$ and Nts^{LH} populations in freely behaving mice that underwent food or water restriction to induce need states and to provoke dynamic ranking

Please cite this article in press as: Petzold et al., Complementary lateral hypothalamic populations resist hunger pressure to balance nutritional and social needs, Cell Metabolism (2023), https://doi.org/10.1016/j.cmet.2023.02.008

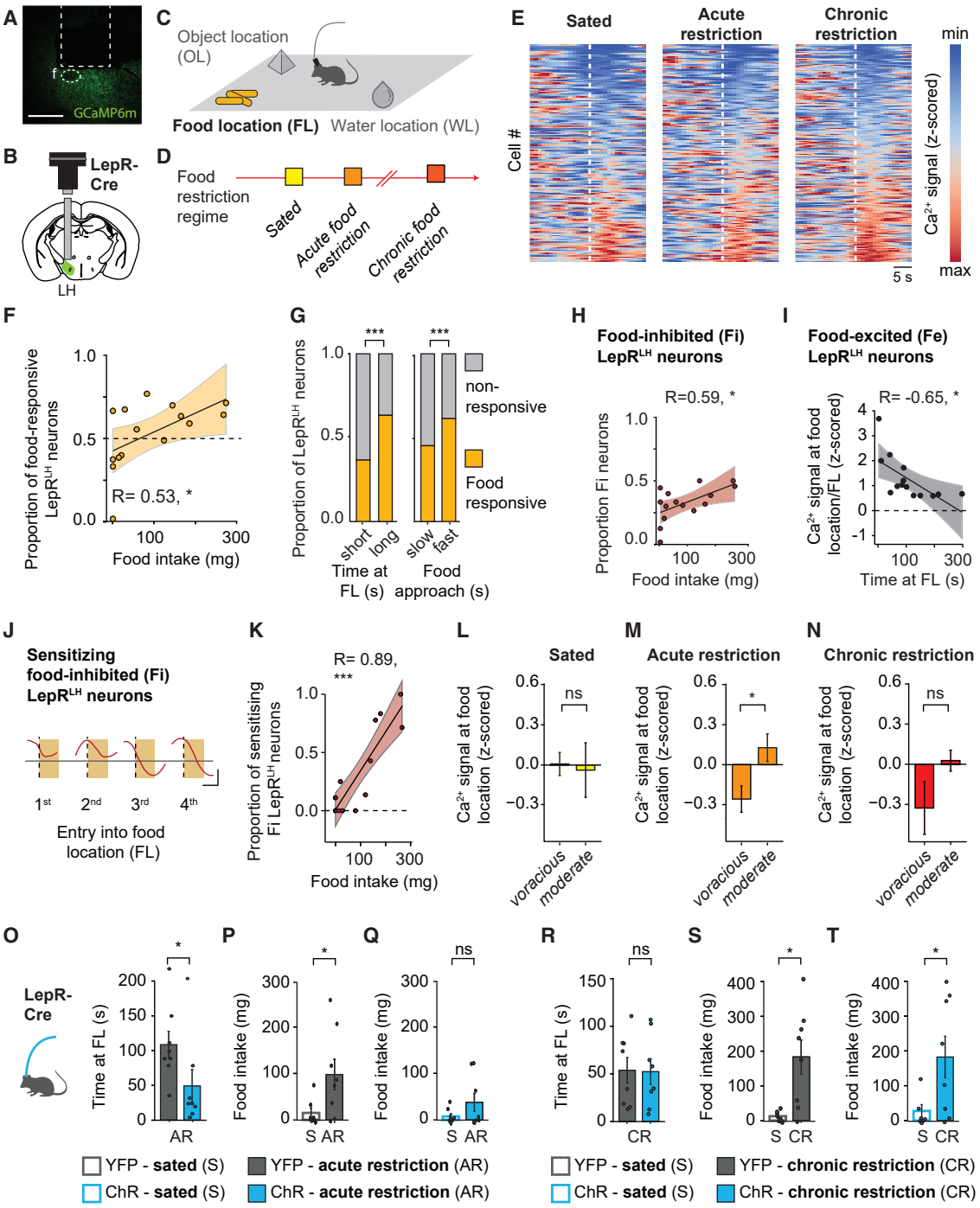

Figure 1. LepR^{LH} neurons track and restrain food intake against hunger pressure

(A) Image of GCaMP6m expression in LepR^{LH} neurons. Dashed line, lens position in LH; f, fornix. Scale bar, 500 μm.

(B) Schema of lens and microendoscope placement.

(C) Enclosure (30 × 50 cm) with free access to a food (FL), water (WL), and object (OL) location for 10 min per session.

(D) Food restriction regime: sated (*ad libitum*), acute restriction (24 h), and chronic restriction (5 days).

(E) Normalized Ca^{2+} signal of recorded neurons sorted by average food-elicited response. Dashed line indicates entry into the food location. Sated, n = 161; acute food restriction, n = 166; chronic food restriction, n = 183 neurons, 5 mice.

(F) Proportion of food-responsive neurons and food intake. n = 261 neurons, 5 mice, 3 imaging days. *p = 0.0415, Pearson's correlation.

(G) Proportion of food-responsive neurons. Left: in mice spending a long or a short time at FL. Right: in mice exhibiting fast and slow food approach. Total, n = 510; food-responsive, n = 261 neurons. 5 mice, 3 imaging days. ***p < 0.001, Pearson's χ^2 test.

(H) Proportion of Fi neurons and food intake. n = 157 neurons, 5 mice, 3 imaging days. *p = 0.0204, Pearson's correlation.

(legend continued on next page)

Please cite this article in press as: Petzold et al., Complementary lateral hypothalamic populations resist hunger pressure to balance nutritional and social needs, Cell Metabolism (2023), https://doi.org/10.1016/j.cmet.2023.02.008

of competing positive stimuli such as potential mates, food, and water. This approach allowed us to specifically determine whether these populations were capable of representing multiple stimuli under different need states. We found that $LepR^{LH}$ and Nts^{LH} populations differentially encode multiple connected as well as competing consumptive stimuli—potential mates, food, and water. Cell-type-specific activation of these populations enabled us to test their functional contribution to the ranking of competing opportunities. Through this integrative approach we discovered that, while both populations track food consumption, leptin-sensitive $LepR^{LH}$ neurons progressively discount food despite hunger pressure to benefit social exploration. Conversely, Nts^{LH} neurons preferentially encode water despite hunger pressure and discount social interaction. Taken together, we provide a mechanistic understanding of how neuronal populations in the LH act in a complementary manner to counteract metabolic pressure in order to relegate feeding and prioritize the pursuit of other highly relevant needs.

RESULTS

Food-elicited inhibition of $LepR^{LH}$ neurons increases with food intake

First, we tested whether leptin receptor-expressing LH ($LepR^{LH}$) neurons were capable of encoding nutritional stimuli in freely behaving animals. We injected the Cre-dependent calcium indicator GCaMP6m into the LH of LepR-Cre mice and implanted a GRIN lens above the LH (Figure 1A) to image the activity of individual $LepR^{LH}$ neurons with a miniaturized endoscope (Figure 1B). During imaging sessions, mice freely explored an enclosure containing food, water, and an object (Figure 1C). To test whether the activity of $LepR^{LH}$ neurons covaried with feeding intensity, we imaged their activity in animals exposed to *ad libitum* access to food ("sated state"), overnight food restriction ("acute restriction state"), or prolonged food restriction across five consecutive days ("chronic restriction state"; Figure 1D). We first analyzed food-elicited activity of $LepR^{LH}$ neurons during spontaneous food exploration (Figure 1E). Across states, we found that a substantial proportion of $LepR^{LH}$ neurons not only responded to food (53%) but that the size of the food-responsive $LepR^{LH}$ population increased with food consumption (Figure 1F). We then assessed food-elicited activity of $LepR^{LH}$ neurons in relation to other feeding-related parameters, including time to approach the food and time spent at the food location (Figures S1A and S1B), and found that the size of the food-responsive $LepR^{LH}$ population correlated with foraging intensity, i.e., animals that spent more time at the food location ("long") or approached food faster ("fast") had a larger population of food-responsive $LepR^{LH}$ neurons (Figure 1G). In contrast, the size of the food-responsive $LepR^{LH}$ population did not correlate with water-seeking intensity (Figure S1C). We also identified water- and object-responsive $LepR^{LH}$ neurons. However, the size of water-responsive or object-responsive $LepR^{LH}$ populations did not correlate with water-seeking or object-exploration intensity (Figures S1D and S1E).

Among food-responsive $LepR^{LH}$ neurons, we identified both food-excited (Figures S1F and S1H) and food-inhibited neurons (Figures S1G and S1H), i.e., neurons whose activity significantly increased or decreased at the food location. Food-excited $LepR^{LH}$ neurons were also activated by all feeding-related behaviors that we tested: food location entry (Figures S1I and S1J), feeding onset (Figures S1K and S1L), and sniffing food (Figures S1M and S1N). Food-inhibited $LepR^{LH}$ neurons responded dynamically to food location entry (Figures S1O and S1P) and were rapidly inhibited by the onset of feeding (Figures S1Q and S1R) rather than just sniffing the food (Figures S1S and S1T).

We next evaluated whether the recruitment of food-excited or food-inhibited $LepR^{LH}$ neurons increased with food intake. Across states, the size of the food-inhibited population increased with food consumption (Figure 1H). In contrast, the size of the food-excited $LepR^{LH}$ population did not correlate with food intake (Figure S2A), and the activity of food-excited cells decreased with the time spent at the food location (Figure 1I). If food-related inhibition of $LepR^{LH}$ neurons facilitated food intake, food-related inhibition may be stronger in fat animals compared to lean ones (Figure S2B). Indeed, food-elicited excitation was dampened (Figure S2C) and food-elicited inhibition was increased (Figure S2D) in fat animals compared to lean ones.

Finally, we analyzed the activity dynamics of $LepR^{LH}$ neurons while animals were able to feed *ad libitum* in a free access enclosure (Figure 1C) to allow satiation. This approach enabled us to evaluate gradual changes of food-elicited responses of individual $LepR^{LH}$ neurons throughout the session (Figure S2E). Indeed, we observed a pronounced change of food-elicited responses in a food-inhibited population: a subpopulation of food-inhibited $LepR^{LH}$ neurons developed stronger food-elicited inhibition

(I) Average activity of Fe neurons and time at FL. n = 104 neurons. As in (H), *p = 0.0115.
(J and K) Sensitizing Fi population.
(J) Example of Ca^{2+} signal during consecutive FL visits.
(K) Proportion and food intake. n = 33 neurons. As in (H), ***p < 0.001.
(L–N) Food-elicited Ca^{2+} signal in voracious and moderate feeders; sample size as in (E).
(L) Sated state: ns, p = 0.86.
(M) Acute restriction: *p = 0.029.
(N) Chronic restriction: ns, p = 0.19, Mann-Whitney U test.
(O–T) Optogenetic activation for 10 min in free access enclosure following acute (O–Q) and chronic (R–T) food restriction. YFP, n = 8 mice; ChR, n = 8 mice.
(O) Time at FL. *p = 0.014, Mann-Whitney U test.
(P and Q) Food intake. YFP, ns, p = 0.14; ChR, *p = 0.035, paired Wilcoxon signed-rank test.
(R) Time at FL. ns, p = 0.33.
(S and T) Food intake. YFP, *p = 0.0355; ChR, *p = 0.036.
Data shown are mean ± SEM. ns, not significant; *p < 0.05, **p < 0.01, ***p < 0.001.
See also Figures S1–S3.

Please cite this article in press as: Petzold et al., Complementary lateral hypothalamic populations resist hunger pressure to balance nutritional and social needs, Cell Metabolism (2023), https://doi.org/10.1016/j.cmet.2023.02.008

during the session (“sensitizing food-inhibited cells”; Figures 1J and S2F). The proportion of this subpopulation increased with food intake (Figure 1K). The proportion of other subpopulations, which changed their food-excitatory responses over the session or reduced their food-inhibitory responses, did not correlate with food intake (Figures S2G–S2M). Taken together, a gradual increase of food-elicited inhibition of $LepR^{LH}$ neurons during a meal accompanies delayed satiation.

$LepR^{LH}$ neurons limit food intake despite acute fasting

In a healthy animal, satiation is matched to energy needs.[32,33] We varied the energy needs of the animals by exposing them to *ad libitum* access to food, or to two different food restriction conditions (Figure 1D). While acute overnight food restriction decreased body weight by around 5% and provoked a mild increase in food intake during refeeding (“feeding rebound”), chronic food restriction over five consecutive days decreased body weight by around 15% and led to a higher feeding rebound (Figures S2N and S2O). Consistent with previous studies in mice[34] and humans,[35] we observed that the extent of the feeding rebound was variable between animals (Figure S2O). If food-elicited inhibition of $LepR^{LH}$ neurons delayed satiation, food-elicited inhibition would be enhanced in animals exhibiting a high feeding rebound. We tested this hypothesis from three perspectives.

We first analyzed how food-elicited inhibition within the $LepR^{LH}$ population changed throughout the imaging session following *ad libitum* access to food or food restriction. We found that, across animals, food-elicited inhibition of $LepR^{LH}$ neurons was enhanced after acute food restriction (Figures S2P and S2Q). We then split mice into two groups according to the extent of the feeding rebound following food restriction (“voracious” and “moderate” feeders; Figure S2R). Neither weight loss (Figure S2S) nor locomotion (Figure S2T) differed between the two groups. Following acute food restriction, “voracious” feeders exhibited stronger food-elicited inhibition of the $LepR^{LH}$ population compared to “moderate” feeders (Figure 1M). We did not detect statistically significant differences in food-elicited responses between “voracious” and “moderate” feeders during *ad libitum* access to food (“sated”; Figure 1L) or following chronic food restriction (Figure 1N).

Finally, we compared the activity of the same individual food-inhibited $LepR^{LH}$ neurons across food restriction states (Figures S3A–S3I). Overall, only around 30% of $LepR^{LH}$ neurons consistently responded to food across all states (Figure S3I), demonstrating state-specific recruitment of $LepR^{LH}$ neurons in food encoding. In “moderate” feeders, neurons that were food-inhibited in the sated state exhibited food-elicited excitation following acute food restriction, but not chronic food restriction (Figures S3J and S3K). In contrast, food-inhibited $LepR^{LH}$ neurons of “voracious” feeders did not exhibit such flexibility (Figures S3L and S3M). Thus, $LepR^{LH}$ neurons can switch from food inhibition to food excitation in animals that eat less despite acute food restriction.

To test whether food-related activation of $LepR^{LH}$ neurons would indeed reduce food intake, we optogenetically activated these neurons during refeeding after acute or chronic food restriction. Activation of $LepR^{LH}$ neurons after acute food restriction reduced the time animals spent at the food location (Figure 1O). We then compared food intake following *ad libitum* access to food (“sated”) and following food restriction. Acute food restriction typically induced a feeding rebound, variable between individuals (Figure 1P). Activation of $LepR^{LH}$ neurons precluded the feeding rebound following acute food restriction (Figure 1Q). However, activation of $LepR^{LH}$ neurons after chronic food restriction did not affect time spent at the food location (Figure 1R), nor did it suppress food intake (Figures 1S, 1T, S3N, and S3O). Taken together, food-elicited excitation of $LepR^{LH}$ neurons may facilitate satiation to suppress feeding despite hunger pressure induced by acute, but not chronic, food restriction.

Leptin activates food-anticipatory $LepR^{LH}$ neurons

A crucial component of the satiation process is the adipose tissue-derived hormone leptin.[36–40] $LepR^{LH}$ neurons respond to leptin *ex vivo*, albeit heterogeneously,[41] implying underlying functional differences within the $LepR^{LH}$ population. To test whether leptin may suppress food intake by stimulating the recruitment of food-responsive $LepR^{LH}$ neurons, we evaluated the relationship between the food-encoding properties of $LepR^{LH}$ neurons and their leptin sensitivity. In agreement with previous studies, a single intraperitoneal (i.p.) injection of leptin acutely suppressed food intake (Figures S4A and S4B). After recording food-elicited responses of $LepR^{LH}$ neurons following acute and chronic food restriction, we let animals regain body weight and measured the response of the same $LepR^{LH}$ neurons to i.p. injection of leptin (in the absence of food) (Figure S4C). This approach allowed us to compare food-elicited responses of the same individual $LepR^{LH}$ neurons with their leptin response (Figure 2A). Strikingly, leptin responses of $LepR^{LH}$ neurons correlated with food-elicited responses measured after acute food restriction (Figure S4E), but not measured after *ad libitum* access to food (“sated”; Figure S4D) or after chronic food restriction (Figure S4F). We then analyzed the response of leptin-activated (Figure 2B) and leptin-suppressed (Figures S4G and S4H) $LepR^{LH}$ neurons to food following different food restriction states. Leptin specifically activated a subgroup of $LepR^{LH}$ neurons that was activated during food approach and rapidly inhibited upon entry into the food location following acute food restriction (Figures 2C and 2D). Leptin did not selectively activate food-anticipatory, food-inhibited $LepR^{LH}$ neurons recruited following *ad libitum* access to food (“sated”; Figure S4I) or chronic food restriction (Figure S4J). Similarly, we did not observe significant food-elicited responses of leptin-suppressed neurons in any of the states that we tested (Figures S4K–S4M). Thus, leptin selectively activates food-anticipatory, food-inhibited $LepR^{LH}$ neurons recruited following acute food restriction.

$LepR^{LH}$ neurons limit water intake despite thirst

Having shown that hunger gates the regulation of feeding by $LepR^{LH}$ neurons, we investigated whether $LepR^{LH}$ neurons encode other nutritional needs. We imaged the activity of $LepR^{LH}$ neurons in animals exploring a free access enclosure containing food, water, and an object following water deprivation to induce a physiological need for water consumption (Figures 3A, S5A, and S5B). We detected a substantial proportion of water-responsive $LepR^{LH}$ neurons even in euhydrated animals

Please cite this article in press as: Petzold et al., Complementary lateral hypothalamic populations resist hunger pressure to balance nutritional and social needs, Cell Metabolism (2023), https://doi.org/10.1016/j.cmet.2023.02.008

CellPress
OPEN ACCESS

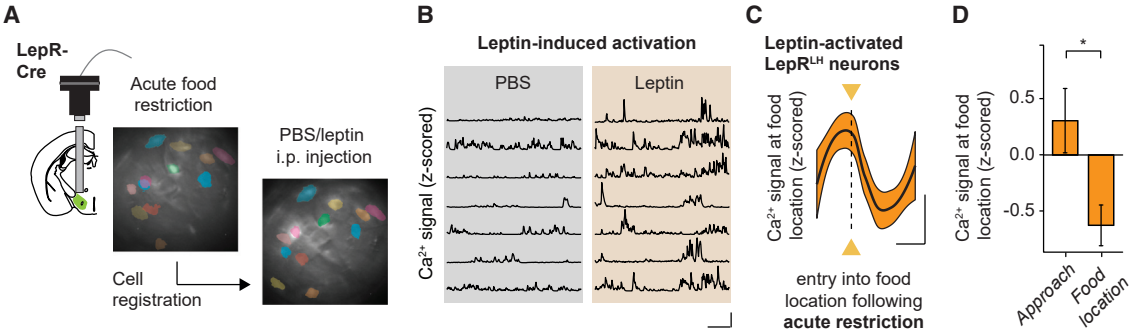

Figure 2. Leptin-mediated recruitment of LepR^{LH} neurons during feeding

(A) Longitudinal registration of neurons imaged across experiments.

(B) Representative Ca^{2+} traces. Scale bar, x = 25 s, y = 0.5 SD.

(C and D) Food-elicited responses of leptin-activated neurons following acute food restriction.

(C) Local fit. Scale bar, x = 10 s, y = 0.4 SD.

(D) Ca^{2+} signal before and after entry into food location. n = 13 neurons, 5 mice. *p = 0.027, paired Wilcoxon signed-rank test.

Data shown are mean ± SEM. *p < 0.05, ***p < 0.001.

See also Figure S4.

("*ad libitum*"; Figure 3B), which increased following water deprivation (Figure 3B). We identified both water-excited (Figures S5C–S5E) and water-inhibited (Figures S5F–S5H) LepR^{LH} neurons. Specifically, water-inhibited neurons were recruited in response to water deprivation (Figure 3C).

To examine if water-related activation of LepR^{LH} neurons suppresses water intake, we activated these neurons optogenetically while animals had *ad libitum* access to water following acute water deprivation. Indeed, optogenetic activation of LepR^{LH} neurons decreased the time animals spent at the water location (Figure 3D) as well as water intake (Figure 3E) despite acute water deprivation. However, it did not affect time spent at the water location following *ad libitum* access to water (Figure S5I) or the time at the food location (Figures S5J and S5K).

Since these findings suggest that water-elicited inhibition among LepR^{LH} neurons facilitates drinking, as food-elicited inhibition facilitates feeding, we directly compared the response of individual LepR^{LH} neurons to deprived needs—food or water—following water or food deprivation (Figure 3F). Across the LepR^{LH} population, each deprived stimulus elicited a similar response magnitude (Figure 3G, inset). Moreover, optogenetic activation of LepR^{LH} neurons led to a reduction of water intake following acute water deprivation that was similar to the reduction of food intake following acute food deprivation (Figure 3H). On a population level, changes in need state from hunger (acute food deprivation) to thirst (acute water deprivation) affect the recruitment of LepR^{LH} neurons that selectively respond to the deprived stimulus ("food-selective" or "water-selective" cells, respectively; Figure S5L). On a single-cell level, 49% of LepR^{LH} neurons recorded during both thirst and hunger states were inhibited by food as well as by water (Figure S5M), underscoring the ability of LepR^{LH} neurons to respond to both food and water in a need-dependent manner.

Food intake under hunger pressure scales water-elicited responses of Nts^{LH} neurons

The need-dependent resistance to feeding and drinking provided by LepR^{LH} neurons is distinct from the role of neurotensin-expressing (Nts^{LH}) neurons in consumptive behavior. Nts^{LH} neurons increase activity in response to thirst,[27] and their activation promotes water intake.[28] Intensification of water-seeking drive would be particularly important in the face of competing physiological pressure—such as hunger—to ensure a healthy balance between eating and drinking (Figure S5N).

To test the possibility that Nts^{LH} neurons complement LepR^{LH} neurons by sustaining water seeking despite competing physiological needs, we first recorded the activity of Nts^{LH} neurons in animals that freely explored the free access enclosure containing food, water, and an object (Figures 4A and 4B) following food and water deprivation. While Nts^{LH} neurons responded to both food and water (Figure 4C), changes in need state from hunger (acute food deprivation) to thirst (acute water deprivation) did not affect the recruitment of Nts^{LH} neurons to food or water encoding (Figure S5O). In contrast to LepR^{LH} neurons (Figure S1D), the size of the water-responsive Nts^{LH} population reflected water-seeking intensity: animals that spent more time at the water location ("long") or approached water faster ("fast") had a larger population of water-responsive Nts^{LH} neurons (Figure 4D). Taken together, these findings indicate that water-related activity of Nts^{LH} neurons facilitates drinking, both in hunger and thirst states.

We then recorded the activity of Nts^{LH} neurons in response to food restriction. Across need states, unlike LepR^{LH} neurons (Figures 1F and 1G), the size of the food-responsive Nts^{LH} population was not related to food intake (Figure S5P) or foraging intensity (Figure S5Q). Moreover, we did not detect a correlation between food-elicited responses and leptin sensitivity of Nts^{LH} neurons across food restriction states (Figures S5R–S5T). However, food restriction affected water encoding by Nts^{LH} neurons (Figure S5U). Similarly, the size of the water-responsive Nts^{LH} population correlated with food intake (Figure 4E), indicating that food consumption specifically modulates water-elicited responses of Nts^{LH} neurons. We then compared the activity of individual Nts^{LH} neurons in response to food and water during acute and chronic food restriction

Please cite this article in press as: Petzold et al., Complementary lateral hypothalamic populations resist hunger pressure to balance nutritional and social needs, Cell Metabolism (2023), https://doi.org/10.1016/j.cmet.2023.02.008

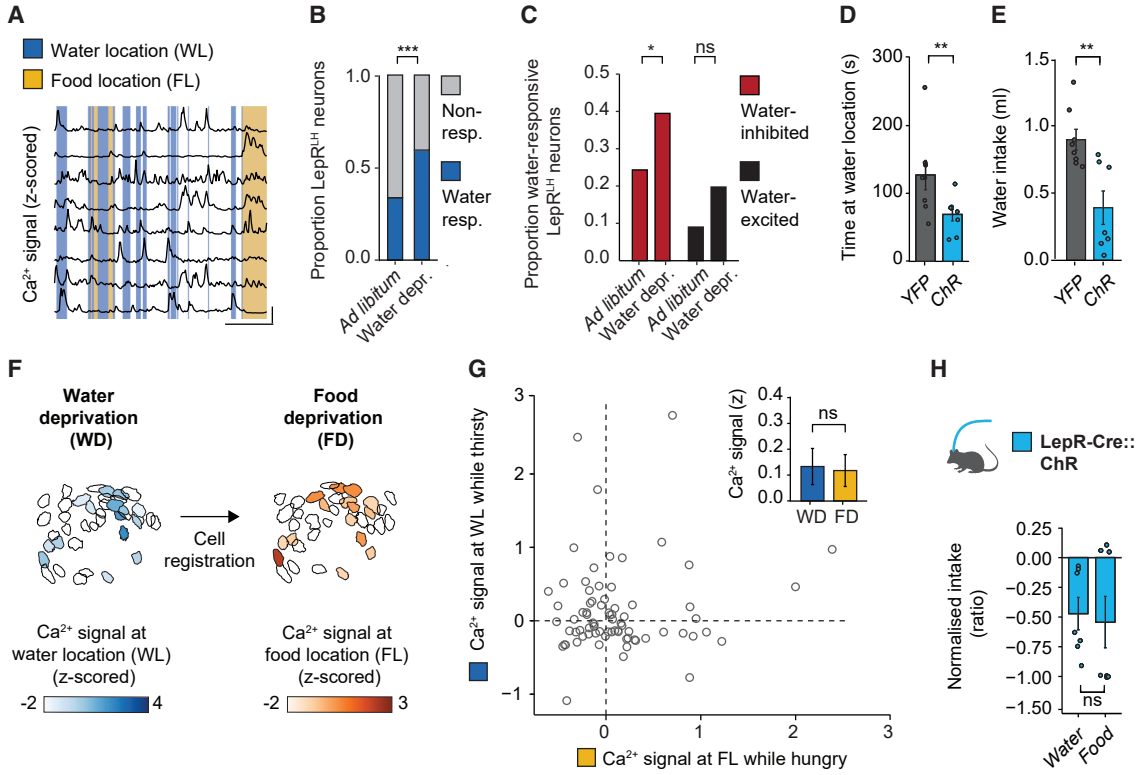

Figure 3. LepR^{LH} neurons limit water intake despite thirst

(A) Representative Ca^{2+} traces. Scale bar, x = 50 s, y = 0.5 SD.

(B) Proportion of neurons responsive to water exposure. Total, n = 263; water-responsive, n = 127 neurons, 5 mice, 2 imaging days. ***p < 0.001, Pearson's χ^2 test.

(C) Proportion of water-excited (We) and water-inhibited neurons (Wi). *Ad libitum*: total, n = 111; We, n = 10; Wi, n = 27; water deprived: total, n = 152; We, n = 30; Wi, n = 60 neurons, 5 mice. ns, p = 0.053; *p = 0.0288, Pearson's χ^2 test for equality of proportions.

(D and E) Optogenetic activation for 10 min in free access enclosure following water deprivation.

(D) Time spent at water location. YFP, n = 8; ChR, n = 8 mice. **p = 0.0094, Mann-Whitney U test.

(E) Water intake. YFP, n = 8; ChR, n = 7 mice. **p = 0.0035, Student's t test.

(F and G) Neural response to deprived stimulus.

(F) Example map of the same neurons detected following acute food or water deprivation. Scale bar reflects amplitude of Ca^{2+} signal at stimulus location.

(G) Response of individual neurons to deprived stimulus following acute food or water deprivation. n = 75 neurons, 5 mice. Inset: ns, p = 0.94; paired Wilcoxon signed-rank test.

(H) Relative intake during 10 min of optogenetic activation in free access enclosure. As in (E), ns, p = 0.43; Mann-Whitney U test.

Data shown are mean ± SEM. ns, not significant; *p < 0.05, **p < 0.01, ***p < 0.001.

See also Figures S5 and S8.

states. Following acute food restriction, Nts^{LH} neurons displayed stronger food than water responses (Figure 4F, left). Conversely, the water response was markedly stronger than the food response following chronic food restriction (Figures 4F, right, and S5V). To investigate the neuronal dynamics underlying this shift in responses to food and water, we specifically examined water-excited and water-inhibited Nts^{LH} neurons following acute and chronic food restriction. The proportion of water-excited Nts^{LH} neurons (Figure 4G) increased following chronic food restriction (Figure 4H) and correlated with food intake (Figure 4I). Concomitantly, the proportion of water-inhibited Nts^{LH} neurons (Figure 4J) decreased following acute and chronic food restriction (Figure 4K) and tended to decrease with food intake (Figure 4L). These coordinated responses suggest that both water-excited and water-inhibited Nts^{LH} neurons track food consumption to promote water intake despite a competing physiological need—hunger.

Nts^{LH} neurons counter hunger pressure to scale water to food intake

Previous studies have shown that the polydipsia induced by activation of Nts^{LH} neurons acutely facilitates feeding following dehydration[28] but reduces feeding after prolonged activation.[31] To test whether the Nts^{LH} population contributes to scaling water to food intake, we chemogenetically activated this population in animals during *ad libitum* access to food and water. All animals were injected i.p. with CNO (1 mg/kg), and we compared water and food intake of animals expressing an excitatory DREADD (hM3Dq) with the intake of animals expressing a control fluorophore (mCherry). In agreement with Kurt et al.,[28] we found that the activation of Nts^{LH} neurons rapidly increased water intake (Figure 5A). While the activation of Nts^{LH} neurons also led to a moderate increase of food intake (Figure 5B), the relative consumption of water was higher compared to food (Figure 5C). Correspondingly, whereas water and food intake are correlated

Please cite this article in press as: Petzold et al., Complementary lateral hypothalamic populations resist hunger pressure to balance nutritional and social needs, Cell Metabolism (2023), https://doi.org/10.1016/j.cmet.2023.02.008

CellPress
OPEN ACCESS

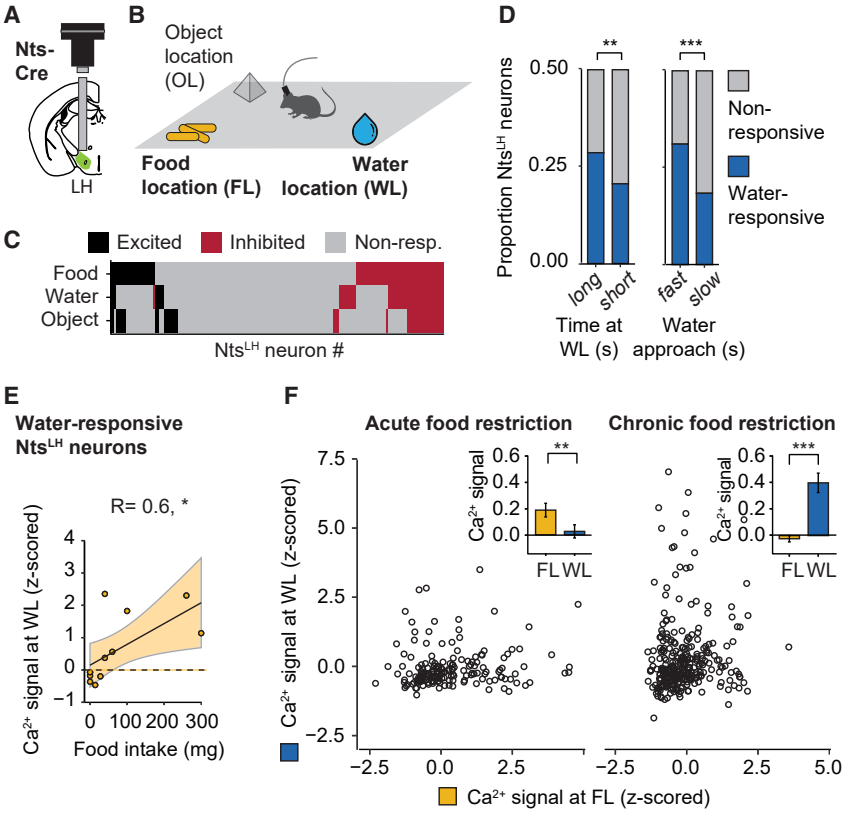

Figure 4. Food intake under hunger pressure scales water-elicited responses of Nts^{LH} neurons

(A) Schema of lens and microendoscope placement.
(B) Enclosure with free access to a food (FL), water (WL), and object (OL) location for 10 min per session.
(C) Stimulus selectivity of individual neurons across three states (following *ad libitum* food access or acute or chronic food restriction). n = 642 neurons.
(D) Proportion of water-responsive neurons. Left: in mice spending a long and a short time at water location (WL). Right: in mice exhibiting fast and slow water approach. n = 853 neurons, 4 mice, 3 imaging days. **p = 0.009, ***p < 0.001, Pearson's χ^2 test.
(E) Food intake and average activity of water-responsive neurons. n = 203 neurons, 4 mice, 3 imaging days. *p = 0.0273, Pearson's correlation.
(F) Activity of individual neurons at WL or FL, 4 mice. Insets: acute restriction, n = 283 neurons, **p = 0.0037; chronic restriction, n = 293 neurons, ***p < 0.001, Wilcoxon signed-rank test.
(G–I) Water-excited (We) neurons.
(G) Representative Ca^{2+} trace.
(H) Proportion across 3 states. ns, p = 1; ***p < 0.001, Pearson's χ^2 test.
(I) Proportion of We neurons and food intake. n = 96 neurons, 4 mice, 3 imaging days. ***p < 0.001, Pearson's correlation.
(J–L) Water-inhibited (Wi) neurons.
(J) As in (G).
(K) As in (H), n = 107 neurons, **p < 0.0079.
(L) As in (I); ns, p = 0.06.
Data shown are mean ± SEM. *p < 0.05, **p < 0.01, ***p < 0.001.
See also Figures S5 and S8.

We then analyzed the activity of Nts^{LH} neurons during different phases of water intake (Figures S6A and S6B). Activity of water-excited Nts^{LH} neurons was increased during all drinking-related behaviors that we tested: water approach (Figures S6C–S6F), drinking (Figures S6C and S6D), and sniffing water (Figures S6E and S6F). Water-inhibited Nts^{LH} neurons were inhibited at the onset of drinking and water sniffing (Figures S6G–S6J). Food-responsive Nts^{LH} neurons did not show anticipatory activity to food (Figures S6K–S6N). Taken together, our results demonstrate that water-excited Nts^{LH} neurons, which respond to both water approach and consumption, are preferentially recruited with increasing food intake (Figure 4), and the activation of Nts^{LH} neurons scales water to food intake by promoting both water approach and consumption (Figure 5).

in control mice (Figure 5D, left), activation of Nts^{LH} neurons disrupted the balance between water and food intake (Figure 5D, right).

To dissect the behavioral components enabling Nts^{LH}-driven water intake, we applied subsecond unsupervised analysis of behavior using motion sequencing (MoSeq; Figure 5E) to automatically extract "syllables"—subsecond components of behavior[42]—while sated and euhydrated animals explored a free access enclosure. Whereas control animals exhibited a similar intensity of water-directed and non-water exploration, chemogenetic activation of Nts^{LH} neurons intensified water-seeking behaviors compared to non-water exploration (Figure 5F), suggesting that activation of Nts^{LH} neurons guides water approach.

LepR^{LH} neurons prioritize social interaction despite hunger pressure

We have shown that food-excited and food-inhibited activity of LepR^{LH} neurons hinders or facilitates feeding, respectively. Surprisingly, we found that i.p. leptin injection did not only acutely suppress feeding (Figures S4A and S4B), but also promoted approach toward a conspecific (Figure 6A) in the presence of

Please cite this article in press as: Petzold et al., Complementary lateral hypothalamic populations resist hunger pressure to balance nutritional and social needs, Cell Metabolism (2023), https://doi.org/10.1016/j.cmet.2023.02.008

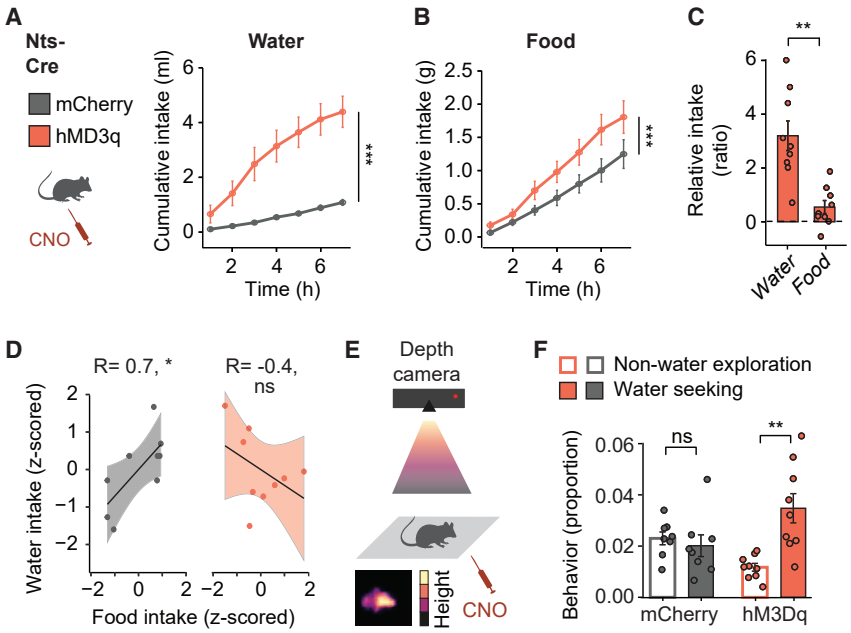

Figure 5. Nts^{LH} neurons promote drinking despite hunger pressure

Chemogenetic activation using CNO (1 mg/kg). Control, n = 9; hM3Dq, n = 9 mice.

(A) Water intake. Group: F(1, 48) = 60, ***p < 0.001, ANOVA.

(B) Food intake. Group: F(1, 48) = 20, ***p < 0.001, ANOVA.

(C) Water or food consumption relative to average consumption of control group. **p = 0.0049, paired t test.

(D) Food and water intake. ns, p = 0.26; *p = 0.0323, Pearson's correlation.

(E) Schematic of motion sequencing (MoSeq) approach.

(F) Usage of water seeking or non-water exploration syllables at water location. ns, p = 0.25; **p = 0.0078, paired Wilcoxon signed-rank test.

Data shown are mean ± SEM. ns, not significant; *p < 0.05, **p < 0.01, ***p < 0.001.

See also Figure S6.

competing nutritional rewards (food and water). While foraging competes with mating and social interaction,[13,43] the neural substrates that balance these innate drives are still elusive. The generalized LepR^{LH}-mediated suppression of consumption despite physiological need may provide a mechanism to integrate social drive with hunger or thirst to determine the hierarchy between those competing needs.

To test this hypothesis, we first assessed whether LepR^{LH} neurons encode social stimuli. We measured the activity levels of LepR^{LH} neurons in male animals that freely explored a free access enclosure containing food, water, and an object, as well as a female conspecific (Figure 6B). Surprisingly, the majority of LepR^{LH} neurons (60%) in male animals responded to interactions with a female (Figure 6C) and the proportion of female-responsive LepR^{LH} neurons increased with the time the animals spent interacting with the female (Figure 6D).

If LepR^{LH} neurons integrate the drive for social contact with drive for feeding, food encoding should interact with the encoding of social stimuli, particularly under hunger pressure. On a single-cell level, we found that a substantial proportion of food-excited (~50%) as well as food-inhibited LepR^{LH} neurons (~70%) was able to encode social stimuli (Figures S7A and S7B). While the food-inhibited neurons, which facilitate feeding, were predominantly inhibited by social stimuli, the food-excited neurons, which decrease feeding, responded to social stimuli heterogeneously (Figure S7A). The size of the food-responsive LepR^{LH} population also increased with food consumption in the presence of a female (Figure S7C), demonstrating that the presence of the female did not prevent LepR^{LH} neurons from tracking food consumption. However, the proportion of social-responsive LepR^{LH} neurons was inversely correlated with food intake (Figure S7D). Similarly, an increase in the proportion of food-responsive LepR^{LH} neurons was associated with a decrease in the proportion of social-responsive LepR^{LH} neurons (Figure 6E). We did not detect a correlation between the size of the social- or food-responsive LepR^{LH} population and the water- or object-responsive LepR^{LH} population (Figures S7E–S7H). While the size of the LepR^{LH} population encoding both food and social stimuli ("Female + Food-responsive" cells; Figure 6F) was stable across need states, we observed a marked increase of food-selective as well as a pronounced decrease of female-selective neurons following food restriction (Figure 6F). Taken together, these findings reveal need-dependent competitive encoding specifically of food and social stimuli by LepR^{LH} neurons.

To evaluate whether LepR^{LH} neurons affect the ranking of food and social stimuli in the context of hunger pressure, we optogenetically stimulated LepR^{LH} neurons in animals that freely explored a free access enclosure containing food, water, an object, and a female conspecific (Figures S7I and S7J). Optogenetic activation of LepR^{LH} neurons following acute, but not chronic, food restriction decreased the time spent at the food location compared to the time of interaction with a female (Figures 6G–6J). To investigate whether the activation of LepR^{LH} neurons shifts the hierarchy of needs, we activated LepR^{LH} neurons optogenetically during simultaneous exposure to food, water, and a female during hunger (acute food deprivation) or thirst (acute water deprivation). While control mice prioritized a female over food and water in the sated state, hunger or thirst shifted the priority away from the female (Figures 6K–6M). In contrast, when LepR^{LH} neurons were activated, animals prioritized the female despite hunger or thirst (Figures 6N–6P). These findings indicate that LepR^{LH} neurons relegate needs for food and water in favor of social interaction despite hunger or thirst.

LepR^{LH} and Nts^{LH} populations exert antagonistic control over social interaction

To evaluate whether LepR^{LH} neurons encode social or specifically sexual stimuli, we analyzed their responses to conspecifics of both sexes. We measured the activity of LepR^{LH} neurons in animals that freely explored an enclosure with two chambers

Please cite this article in press as: Petzold et al., Complementary lateral hypothalamic populations resist hunger pressure to balance nutritional and social needs, Cell Metabolism (2023), https://doi.org/10.1016/j.cmet.2023.02.008

CellPress
OPEN ACCESS

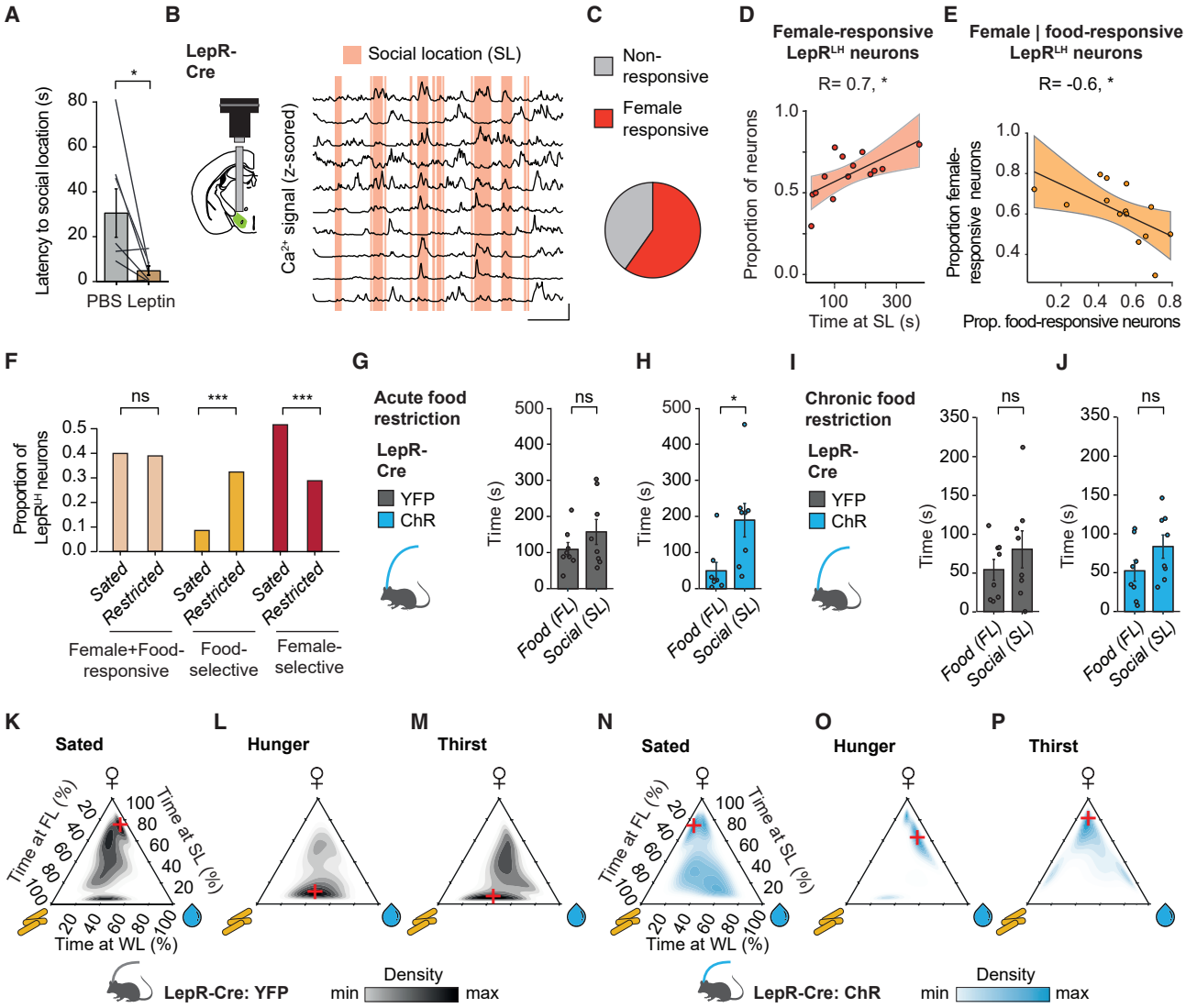

Figure 6. LepR^{LH} neurons prioritize social interaction despite hunger pressure

(A) Latency to social location 30 min after i.p. leptin injection. n = 7 mice. *p = 0.036, paired Wilcoxon signed-rank test.

(B) Schema of lens and microendoscope placement and representative Ca^{2+} traces. Scale bar, x = 50 s, y = 0.5 SD.

(C) Proportion of female-responsive neurons. Total, n = 460; female-responsive, n = 275 neurons. 5 mice, 3 imaging days. ***p < 0.001, χ^2 test for given probabilities.

(D) Proportion of female-responsive neurons and time at SL. n = 275 neurons, 5 mice, 3 imaging days. *p = 0.0101, Pearson's correlation.

(E) Proportion of female- and food-responsive neurons. n = 5 mice, 3 imaging days. *p = 0.022, Pearson's correlation.

(F) Proportion of stimulus-selective neurons. Sated: n = 93 neurons, 5 mice, 1 imaging day. Restricted: n = 281, 5 mice, 2 imaging days. ns, p = 0.9618; ***p < 0.001, χ^2 test for equality of proportions.

(G and H) Time at SL or FL during optogenetic activation in the free access enclosure for 10 min per session following acute restriction.

(G) YFP: n = 8 mice; ns, p = 0.64.

(H) ChR: n = 8 mice, *p = 0.039.

(I and J) As in (G) and (H) following chronic food restriction. ns, p > 0.38, paired Wilcoxon signed-rank test.

(K–P) Time spent at stimulus locations in the free access enclosure during 10 min per session (top corner, SL; left corner, FL; right corner, WL) during optogenetic activation in sated state and following water or food deprivation. YFP, n = 8; ChR, n = 8 mice. Red cross indicates peak of density estimation.

Data shown are mean ± SEM. ns, not significant; *p < 0.05, **p < 0.01, ***p < 0.001.

See also Figure S7.

that contained either male or female conspecifics separated by a central chamber (Figures 7A and 7B). Surprisingly, LepR^{LH} neurons of males exhibited stronger excitation during interaction with females compared to males (Figures 7C and 7D). In female mice, LepR^{LH} neurons exhibited stronger excitation during interaction with males compared to females (Figures S7K and S7L).

Conspecific-related activation of LepR^{LH} neurons may affect social drive in a sex-selective manner. Thus, we optogenetically

Please cite this article in press as: Petzold et al., Complementary lateral hypothalamic populations resist hunger pressure to balance nutritional and social needs, Cell Metabolism (2023), https://doi.org/10.1016/j.cmet.2023.02.008

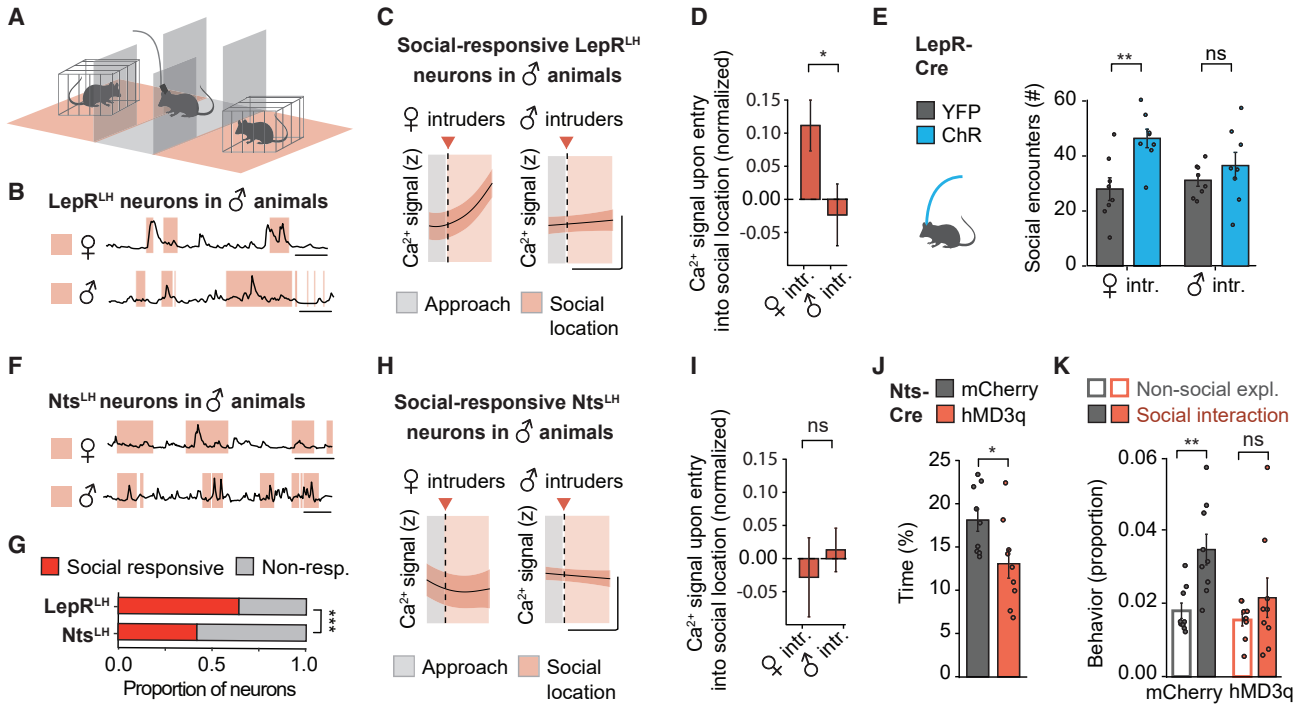

Figure 7. LepR^{LH} and Nts^{LH} populations exert antagonistic control over social interaction

(A) Access to two conspecifics placed behind a mesh.

(B) Representative Ca^{2+} traces of social-responsive LepR^{LH} neurons. Scale bar, 25 s.

(C) Ca^{2+} signal around entry (dashed line) into SL. Female intruders' session, n = 82 neurons, 5 mice; male intruders' session, n = 113 neurons, 6 mice, GAM fit. Scale bar, x = 5 s, y = 0.2 SD.

(D) Ca^{2+} signal upon entry into social location, normalized to approach phase. *p = 0.0357, Mann-Whitney U test.

(E) Optogenetic activation of LepR^{LH} neurons and social exploration. YFP, n = 8 mice; ChR, n = 8 mice. ns, p = 0.32; **p = 0.0038, Student's t test.

(F) Representative Ca^{2+} traces of social-responsive Nts^{LH} neurons. Scale bar, 25 s.

(G) Proportion of social-responsive neurons. LepR^{LH}: total, n = 314; social-responsive, n = 207 neurons, 6 mice, 2 imaging days; Nts^{LH}: total, n = 179; social-responsive, n = 75 neurons, 2 mice, 2 imaging days; LepR^{LH} - Nts^{LH}, ***p < 0.001, Pearson's χ^2 test.

(H) As in (C) for Nts^{LH} neurons. Female intruders' session, n = 72 neurons, 2 mice; male intruders' session, n = 60 neurons, 2 mice.

(I) As in (D) for Nts^{LH} neurons. ns, p = 0.14.

(J and K) Chemogenetic activation of Nts^{LH} neurons using CNO (1 mg/kg). Control, n = 9 mice; hM3Dq, n = 9 mice.

(J) Social exploration. *p = 0.0294, Student's t test.

(K) Usage of social exploration syllables at SL identified using MoSeq. **p = 0.0078; ns, p = 1; paired Wilcoxon signed-rank test with Bonferroni correction.

Data shown are mean ± SEM. *p < 0.05, **p < 0.01, ***p < 0.001.

See also Figures S7 and S8.

activated LepR^{LH} neurons while animals explored the enclosure containing two male or female conspecifics (Figure 7A). Indeed, optogenetic stimulation of LepR^{LH} neurons increased interaction with females, but not with males (Figure 7E), without affecting overall activity levels (Figure S7M). Thus, LepR^{LH} neurons of both males and females differentiate between the sexes and promote interaction with females, suggesting that LepR^{LH} neurons may contribute to guiding sexual drive.

We also studied the role of Nts^{LH} neurons in social interactions as this population regulates other appetitive behaviors in a manner distinct from LepR^{LH} neurons (Figures 4 and 5). First, we measured the activity of Nts^{LH} neurons in animals that explored the enclosure containing two male or female conspecifics (Figures 7A and 7F). While a substantial proportion of Nts^{LH} neurons responded to social stimuli, this population was smaller than the LepR^{LH} population (Figure 7G). In contrast to LepR^{LH} neurons, Nts^{LH} neurons did not differentiate between the sexes (Figures 7H and 7I). Furthermore, chemogenetic activation of Nts^{LH} neurons reduced social interaction (Figure 7J) without affecting overall activity levels (Figure S7N). To investigate exploratory behaviors in the vicinity of a conspecific at a precise timescale, we applied MoSeq (Figure 5E). While control animals preferentially engaged in social interaction compared to non-social exploration, chemogenetic activation of Nts^{LH} neurons disrupted this preference (Figures 7K and S7O). Thus, LepR^{LH} and Nts^{LH} populations exert opposite effects on social interaction, with LepR^{LH} neurons promoting social drive in a sex-specific manner and Nts^{LH} neurons restraining social drive.

Multimodal responses of LepR^{LH} and Nts^{LH} neurons to nutritional and non-nutritional rewards

LepR^{LH} and Nts^{LH} populations encoded multiple nutritional and non-nutritional stimuli (i.e., food, water, an object, and/or a conspecific; Figure S8A). The proportion of neurons exclusively

Please cite this article in press as: Petzold et al., Complementary lateral hypothalamic populations resist hunger pressure to balance nutritional and social needs, Cell Metabolism (2023), https://doi.org/10.1016/j.cmet.2023.02.008

responsive to one stimulus was larger among Nts^{LH} neurons (44%) in comparison to $LepR^{LH}$ neurons (34%; Figure S8A).

In the LH, expression of LepR and Nts partly overlaps.[44–46] To analyze the functional overlap between Nts^{LH} and $LepR^{LH}$ neurons, we assessed the distribution of reward-elicited responses across both populations. The stimulus-elicited activity of both populations revealed a multimodal distribution comprised of three underlying functional subpopulations following food deprivation (Figures S8B–S8D): the food-inhibited subpopulation centered at the first estimated mode (−0.4 SD) was dominated by $LepR^{LH}$ neurons, and the food-excited subpopulation centered at the second estimated mode (0.9 SD) was dominated by Nts^{LH} neurons (Figure S8B). Those Nts^{LH} neurons that showed food-inhibited responses similar to the $LepR^{LH}$ population (64%; Figure S8B) could reflect the overlapping population of Nts+ LepR+ LH neurons. Water-elicited responses followed a multimodal distribution as well (Figure S8C): a moderately water-inhibited subpopulation (mode at −0.5 SD) was dominated by $LepR^{LH}$ neurons and a water-excited subpopulation (mode at 0.9 SD) was dominated by Nts^{LH} neurons, as well as an extremely water-excited subpopulation that was only detected among Nts^{LH} neurons. The population with overlapping water-elicited responses comprised 28% (Figure S8C). Similarly, analysis of conspecific-elicited responses of $LepR^{LH}$ and Nts^{LH} neurons followed a multimodal distribution, with an overlap of 55% (Figure S8D). These findings suggest a partial overlap of stimulus-elicited responses of both populations, consistent with a partial anatomical overlap.[44,45]

DISCUSSION

Here, we show that LH populations enable animals to resist metabolic pressure to relegate nutritional needs in favor of social needs, thereby providing protection against overeating and ensuring behavioral flexibility.

A leptin-sensitive LH population limits hunger pressure in a state-dependent manner and at a fast timescale

The adipokine leptin acts as a signal in a negative feedback loop to scale feeding to physiological need.[39] During fasting, leptin levels decrease, which increases the drive to feed.[47] Classical studies demonstrated the crucial role of leptin in the control of body weight through systemic leptin injection into leptin-deficient mice, which alleviated their obese phenotype.[36–38] In fasted lean humans, leptin levels measured directly before a meal negatively correlate with meal size.[48] In mice, we found that systemic leptin injection acutely suppressed food intake in the course of a meal. While brain-wide loss of LepR expression leads to hyperphagia and weight gain,[49] brain-specific expression of LepR reduces these symptoms in LepR-deficient mice.[50] Leptin infusion directly into the LH lowers body weight and suppresses feeding,[18,41] whereas loss of LepR in LH neurons leads to hyperphagia and weight gain.[25] We hypothesized that the $LepR^{LH}$ population limits fasting-induced refeeding to relegate nutritional needs.

Using single-cell Ca^{2+} imaging in freely behaving mice, we showed that $LepR^{LH}$ neurons tracked food intake. We identified an $LepR^{LH}$ subpopulation that exhibited escalating food-elicited inhibition in fasted animals in the course of a meal. The activation of $LepR^{LH}$ neurons decreased the time that fasted animals spent near the food and precluded fasting-induced refeeding. These data demonstrate that $LepR^{LH}$ neurons continuously evaluate food intake to limit meal size.

In our experiments, we applied a food restriction regime to decrease energy stores and induce hunger. While acute food restriction led to a modest average body weight reduction of 5% that is likely due to the absence of food from the gastrointestinal tract, chronic food restriction led to an average body weight reduction of 15%. By varying the hunger state of the animals, we found that food-elicited inhibition among $LepR^{LH}$ neurons was enhanced specifically following acute food restriction, but not following *ad libitum* access to food or chronic food restriction. While food-elicited inhibition of the $LepR^{LH}$ population generally increased with food intake in the course of a meal, it was enhanced in animals that exhibited a high feeding rebound specifically following acute food restriction. Similarly, activation of $LepR^{LH}$ neurons precluded a feeding rebound induced only by acute food restriction. The extent of the feeding rebound suppression during activation of $LepR^{LH}$ neurons was variable between individuals, which indicates that acute food restriction did not affect all animals to the same degree. Future studies should evaluate how interindividual differences in response to fasting gate $LepR^{LH}$-mediated refeeding.

Furthermore, we identified a leptin-activated subpopulation of $LepR^{LH}$ neurons that was excited during food approach and rapidly inhibited upon entry into the food location. This subgroup was recruited specifically following acute, but not following chronic food restriction or *ad libitum* access to food. This subpopulation may prevent the onset of a feeding bout and could provide a potential substrate for leptin-mediated satiation to limit over-feeding specifically after acute fasting.

Differences in need state could gate $LepR^{LH}$-mediated refeeding through other hunger-sensitive circuits. For instance, hunger-signaling agouti-related peptide (AgRP) neurons of the arcuate nucleus in the medial hypothalamus intensify food seeking and feeding,[51,52] at least in part through LH projections.[4] AgRP neurons are GABAergic[53] and inhibit glutamatergic LH neurons to delay satiation and promote feeding.[54,55] Acute fasting activates AgRP neurons,[56] which may decrease the overall excitatory tone onto GABAergic LH neurons that the $LepR^{LH}$ population is part of,[46] to delay satiation. Prolonged fasting triggers a stress response and further enhances excitability of AgRP neurons,[57] which may sustain the suppression of $LepR^{LH}$ populations during refeeding as a protective mechanism to sustain food intake at times of starvation. *Ex vivo* studies[41] as well as our *in vivo* study demonstrate that the response of $LepR^{LH}$ neurons to leptin is heterogeneous. Previous studies found that an increase in leptin sensitivity of LepR neurons suppresses refeeding following fasting, but not in the sated state,[58] indicating that the contribution of leptin-sensitive LH neurons to the regulation of feeding is state-dependent. Taken together, acute fasting may provide a critical window for leptin-mediated suppression of feeding through interacting medial and lateral hypothalamic circuits.

The ability to suppress physiological needs enables some humans to lose weight by restricting their diet. However, diets often fail due to the inability to resist hunger pressure. Even initial successful weight loss is endangered by the "yo-yo effect"

Please cite this article in press as: Petzold et al., Complementary lateral hypothalamic populations resist hunger pressure to balance nutritional and social needs, Cell Metabolism (2023), https://doi.org/10.1016/j.cmet.2023.02.008

provoked by the diet-induced energy deficit.[40,59] The susceptibility of the negative feedback loop between LepR^{LH} activity, sensitivity of LepR^{LH} cells to leptin, and food consumption to hunger pressure could provide a therapeutic target for diet intervention to circumvent a fasting-induced eating rebound.

Complementary LH populations balance nutritional needs

Systemic leptin injection reduces not only food intake[36,37] but also water intake,[38] and electrolytic lesion of the LH disrupts feeding[12] as well as drinking.[60] While the LH is thought to integrate metabolic needs and motivated behavior,[15,16,61] no studies to date have demonstrated that distinct LH populations track multiple metabolic needs and balance motivated behaviors accordingly, although it is essential for an animal to continuously evaluate multiple needs according to state and opportunity.

In this context, we found that LepR^{LH} neurons encoded multiple innate rewards, such as food and water, in a state-dependent manner. Furthermore, we found that water-related activation of LepR^{LH} neurons reduced drinking, similar to food-related activation, which reduced feeding, demonstrating that LepR^{LH} neurons regulate the pursuit of multiple nutritional rewards.

We also observed water-elicited responses in Nts^{LH} neurons, which are known to be sensitive to thirst.[27] Nts^{LH} neurons exhibited enhanced water responses especially after prolonged fasting. In addition, Nts^{LH} neurons were activated during water approach and their activation facilitated water exploration, suggesting that Nts^{LH} neurons support the anticipatory phase of need fulfilment. In contrast to the LepR^{LH} population, and in agreement with previous studies,[28–31] we observed increased water intake when activating Nts^{LH} neurons. In previous studies, when Nts^{LH} neurons were activated during the light phase, the activation promoted water intake without affecting food intake in euhydrated, sated animals,[28,29,31] as well as in thirsty animals,[28,29] and increased intake of palatable liquid over water.[28,29] The polydipsia induced by activation of Nts^{LH} neurons reinstates feeding after dehydration.[28] Similarly, polydipsia due to activation of Nts^{LH} neurons during the light phase reduces feeding in the dark phase in sated animals.[31] In hungry animals, activation of Nts^{LH} neurons in the beginning of the light and dark phase increased water intake in the light phase and food intake in the dark phase.[29] Interestingly, constitutive loss of neurotensin receptor 1 (NtsR1) decreases intake of normal food, but increases intake of palatable food specifically in the dark phase.[62] These observations suggest that the deprivation state of the animal, as well as circadian rhythms and hedonic value of the nutrient, shape the regulation of ingestive behaviors by Nts^{LH} neurons. We chemogenetically activated Nts^{LH} neurons in the beginning of the dark phase and measured food and water consumption in parallel in animals that were not food or water deprived. Under these conditions, we observed a modest increase in food intake along with a strong increase in water intake.

Importantly, between ~16% and 30% of Nts^{LH} neurons co-express LepR.[27,44,45] Loss of LepR in Nts^{LH} neurons does not affect water intake,[45] suggesting that this subgroup does not contribute to the water-promoting role of Nts^{LH} neurons. Whereas loss of LepR in Nts neurons does not affect food intake in sated mice,[45] it prevents the direct activation of Nts neurons by leptin *in vitro*.[44] Accordingly, mice lacking LepR in Nts^{LH} neurons do not reduce food intake in response to leptin injection,[45] implying that LepR + Nts^{LH} neurons may scale the hedonic value of nutrients.

Taken together, both LepR^{LH} and Nts^{LH} neurons encoded both food and water during hunger as well as during thirst, but both populations had distinct roles in their prioritization. While LepR^{LH} neurons tracked food intake to restrain feeding and tracked water intake to restrain drinking, Nts^{LH} neurons tracked food intake to promote drinking despite strong hunger pressure. Nts^{LH} neurons responded to water most strongly following chronic food restriction, which may provide a feedback loop that balances food and water intake against a strong hunger drive. Such cooperation between LepR^{LH} and Nts^{LH} neurons to drinking is akin to the cooperation between AgRP and proopiomelanocortin (POMC) neurons of the arcuate nucleus to feeding.[51,63] These findings have important implications for the treatment of patients with obesity who often fail to recognize thirst and eat instead, thereby adding to their caloric intake and, ultimately, further weight gain.

Integration of nutritional and social needs by LH populations

Food or water deprivation induces nutritional needs, which compete with social drive. For instance, the presence of a potential mate decreases food consumption of hungry male or female mice. Conversely, prolonged fasting decreases mating behaviors of males as well as females.[13] Leptin injection alleviates the fasting-induced neuroendocrine starvation response, including the increased secretion of stress hormones and decreased secretion of sex hormones,[64] implying a contribution of leptin signaling to reproductive behaviors.[47]

Systemic leptin injection facilitates reproductive behaviors in rodents.[65] In agreement, we found that systemic leptin injection promoted social exploration. However, the neural pathways linking leptin signaling to the expression of socio-sexual behavior are still elusive. Here we found that the LepR^{LH} population relegates nutritional needs in favor of social needs despite hunger or thirst pressure. LepR^{LH} neurons preferentially encoded potential mating partners and promoted the pursuit of females despite food or water deprivation. LepR^{LH} neurons project to lateral hypothalamic orexin (OX)/hypocretin neurons,[66] which mediate stress responses[67,68] including stress responses to hunger.[69] The activation of LepR^{LH} neurons or systemic leptin injection reduces OX-mediated stress responses,[69] although OX neurons do not express leptin receptors.[18,46,66] The prioritization of social over metabolic needs may be mediated by suppression of the hunger-induced stress response via direct input of leptin-sensitive LepR^{LH} neurons to OX neurons.

In contrast to the LepR^{LH} population, Nts^{LH} neurons did not distinguish between the sex of conspecifics and suppressed social exploration. Similar to feeding and drinking, LepR^{LH} and Nts^{LH} neurons play opposite roles in the regulation of social behavior.

Hunger and thirst provide strong drives to motivate eating and drinking, which are essential behaviors to ensure survival. However, animals need to be able to temporarily resist the drive to feed or drink to explore competing opportunities such as potential mates. We show that individual neuronal populations of the LH track multiple needs, coordinate their fulfillment, and weigh

up competing stimuli to enable the pursuit of opportunities against metabolic pressure. Decoupling of reward seeking from current metabolic demands is a double-edged sword. While it ensures behavioral flexibility, i.e., the pursuit of an attractive opportunity despite acute metabolic pressure, it also endangers homeostasis: impairments of multiple innate behaviors aimed at fulfilling essential nutritional and social needs accompany a manifold of neuropsychiatric disorders. Whereas individuals with autism spectrum disorders often exhibit nutritional challenges, including selective eating patterns and food neophobia,[70] persons with anorexia and bulimia nervosa frequently suffer from social phobia.[71] We suggest that the prioritization of social and nutritional needs against acute metabolic pressure by complementary neural populations of the LH makes them a promising target for the development of new therapies.

Limitations of study

We provide strong evidence for the complementary role of two LH populations in the hunger-resistant regulation of feeding and drinking-related behaviors. Both populations also express other neurotransmitters and receptors, which may modulate their functions. While Cre lines are tremendously helpful to obtain neurochemical specificity, they cannot capture the intersectional heterogeneity of LH populations. This would be useful for investigating effects of neural activity changes of such functionally heterogeneous populations such as $LepR^{LH}$ neurons. In our opto- and chemogenetic experiments, we stimulated $LepR^{LH}$ or Nts^{LH} neurons, irrespective of their individual, spontaneous activity profile. Future studies combining Ca^{2+} imaging with gene expression profiling using spatial transcriptomics[72] could relate the behavior-dependent activity of individual LH neurons with their molecular profile and potentially allow the targeting of functional subgroups for selective modulation of their activity.

Additionally, since disruption of either LH population may pose a risk factor for the development of obesity, it will be important for future studies to evaluate long-term changes in the activity profile of individual $LepR^{LH}$ and Nts^{LH} neurons throughout the development of obesity in animals chronically exposed to a high-fat diet.

STAR★METHODS

Detailed methods are provided in the online version of this paper and include the following:

- KEY RESOURCES TABLE
- RESOURCE AVAILABILITY
  - Lead contact
  - Materials availability
  - Data and code availability
- EXPERIMENTAL MODEL AND SUBJECT DETAILS
- METHOD DETAILS
  - Surgical procedures
  - Deep brain single-cell imaging
  - Optogenetic stimulation and data acquisition
  - Chemogenetic stimulation and data acquisition
  - Behavioral assays
  - Pharmacological assays
  - Histology
  - Behavioral scoring
- QUANTIFICATION AND STATISTICAL ANALYSIS
  - Data analysis
  - Statistical analysis

SUPPLEMENTAL INFORMATION

Supplemental information can be found online at https://doi.org/10.1016/j.cmet.2023.02.008.

ACKNOWLEDGMENTS

We gratefully acknowledge support by the ERC Consolidator Grant (772994, FeedHypNet, to T.K.), the Deutsche Forschungsgemeinschaft (German Research Foundation, project ID 431549029 – SFB 1451 to T.K.; EXC2030 CECAD to T.K.; and 233886668-GRK1960 to R.F.-S.), and Center for Molecular Medicine (CMMC), Cologne, to T.K. We also thank Dr. Stefan Vollmar and his team, as well as Dr. Peter Heger and the *Regionales Rechenzentrum* (RRZK) team, for their valuable IT support; Dr. Karl Deisseroth and Dr. Bryan Roth for source plasmids; Dr. Sandeep Robert Datta with Ralph Peterson and Winthrop Gillis for making their MoSeq code available and providing support for further analysis; Dr. Garret Stuber and Randall L. Ung for adapting the MoSeq code to Python; Dr. Oliver Barnstedt for his assistance in data pre-processing; and Dr. Jens C. Brüning, Dr. Sophie Steculorum, and Dr. Silvana Valtcheva for fruitful discussions.

AUTHOR CONTRIBUTIONS

A.P. and T.K. designed the experiments; A.P. performed *in vivo* calcium imaging experiments; H.E.v.d.M. performed chemogenetic and MoSeq experiments; R.F.-S. performed optogenetic experiments and *in vivo* calcium imaging experiments for Figures S7K and S7L; A.P. performed data analysis except for MoSeq experiments (H.E.v.d.M.); T.K. supervised the study; and A.P. and T.K. wrote the manuscript with input from all authors.

DECLARATION OF INTERESTS

The authors declare no competing interests.

Received: November 15, 2021
Revised: May 3, 2022
Accepted: February 8, 2023
Published: February 23, 2023

REFERENCES

1. Betley, J.N., Xu, S., Cao, Z.F.H., Gong, R., Magnus, C.J., Yu, Y., and Sternson, S.M. (2015). Neurons for hunger and thirst transmit a negative-valence teaching signal. Nature *521*, 180–185. https://doi.org/10.1038/nature14416.
2. Dietrich, M.O., Zimmer, M.R., Bober, J., and Horvath, T.L. (2015). Hypothalamic Agrp neurons drive stereotypic behaviors beyond feeding. Cell *160*, 1222–1232. https://doi.org/10.1016/j.cell.2015.02.024.
3. Jennings, J.H., Ung, R.L., Resendez, S.L., Stamatakis, A.M., Taylor, J.G., Huang, J., Veleta, K., Kantak, P.A., Aita, M., Shilling-Scrivo, K., et al. (2015). Visualizing hypothalamic network dynamics for appetitive and consummatory behaviors. Cell *160*, 516–527. https://doi.org/10.1016/j.cell.2014.12.026.
4. Steculorum, S.M., Ruud, J., Karakasilioti, I., Backes, H., Engström Ruud, L., Timper, K., Hess, M.E., Tsaousidou, E., Mauer, J., Vogt, M.C., et al. (2016). AgRP neurons control systemic insulin sensitivity via myostatin expression in brown adipose tissue. Cell *165*, 125–138. https://doi.org/10.1016/j.cell.2016.02.044.
5. Carus-Cadavieco, M., Gorbati, M., Ye, L., Bender, F., Van Der Veldt, S., Kosse, C., Börgers, C., Lee, S.Y., Ramakrishnan, C., Hu, Y., et al. (2017). Gamma oscillations organize top-down signalling to hypothalamus

and enable food seeking. Nature *542*, 232–236. https://doi.org/10.1038/nature21066.

6. Zimmerman, C.A., Lin, Y.-C., Leib, D.E., Guo, L., Huey, E.L., Daly, G.E., Chen, Y., and Knight, Z.A. (2016). Thirst neurons anticipate the homeostatic consequences of eating and drinking. Nature *537*, 680–684. https://doi.org/10.1038/nature18950.
7. Allen, W.E., DeNardo, L.A., Chen, M.Z., Liu, C.D., Loh, K.M., Fenno, L.E., Ramakrishnan, C., Deisseroth, K., and Luo, L. (2017). Thirst-associated preoptic neurons encode an aversive motivational drive. Science *357*, 1149–1155. https://doi.org/10.1126/science.aan6747.
8. McHenry, J.A., Otis, J.M., Rossi, M.A., Robinson, J.E., Kosyk, O., Miller, N.W., McElligott, Z.A., Budygin, E.A., Rubinow, D.R., and Stuber, G.D. (2017). Hormonal gain control of a medial preoptic area social reward circuit. Nat. Neurosci. *20*, 449–458. https://doi.org/10.1038/nn.4487.
9. Karigo, T., Kennedy, A., Yang, B., Liu, M., Tai, D., Wahle, I.A., and Anderson, D.J. (2021). Distinct hypothalamic control of same- and opposite-sex mounting behaviour in mice. Nature *589*, 258–263. https://doi.org/10.1038/s41586-020-2995-0.
10. Yoon, H., Enquist, L.W., and Dulac, C. (2005). Olfactory inputs to hypothalamic neurons controlling reproduction and fertility. Cell *123*, 669–682. https://doi.org/10.1016/j.cell.2005.08.039.
11. Verplanck, W.S., and Hayes, J.R. (1953). Eating and drinking as a function of maintenance schedule. J. Comp. Physiol. Psychol. *46*, 327–333. https://doi.org/10.1037/h0055380.
12. Anand, B.K., and Brobeck, J.R. (1951). Hypothalamic control of food intake in rats and cats. Yale J. Biol. Med. *24*, 123–140.
13. Burnett, C.J., Funderburk, S.C., Navarrete, J., Sabol, A., Liang-Guallpa, J., Desrochers, T.M., and Krashes, M.J. (2019). Need-based prioritization of behavior. eLife *8*, 44527. https://doi.org/10.7554/eLife.44527.
14. Wade, G.N., and Schneider, J.E. (1992). Metabolic fuels and reproduction in female mammals. Neurosci. Biobehav. Rev. *16*, 235–272. https://doi.org/10.1016/S0149-7634(05)80183-6.
15. Sternson, S.M., and Eiselt, A.K. (2017). Three pillars for the neural control of appetite. Annu. Rev. Physiol. *79*, 401–423. https://doi.org/10.1146/annurev-physiol-021115-104948.
16. Stuber, G.D., and Wise, R.A. (2016). Lateral hypothalamic circuits for feeding and reward. Nat. Neurosci. *19*, 198–205. https://doi.org/10.1038/nn.4220.
17. Bonnavion, P., Mickelsen, L.E., Fujita, A., de Lecea, L., and Jackson, A.C. (2016). Hubs and spokes of the lateral hypothalamus: cell types, circuits and behaviour. J. Physiol. *594*, 6443–6462. https://doi.org/10.1113/JP271946.
18. Laque, A., Zhang, Y., Gettys, S., Nguyen, T.A., Bui, K., Morrison, C.D., and Münzberg, H. (2013). Leptin receptor neurons in the mouse hypothalamus are colocalized with the neuropeptide galanin and mediate anorexigenic leptin action. Am. J. Physiol. Endocrinol. Metab. *304*, 999–1011. https://doi.org/10.1152/ajpendo.00643.2012.
19. Jennings, J.H., Rizzi, G., Stamatakis, A.M., Ung, R.L., and Stuber, G.D. (2013). The inhibitory circuit architecture of the lateral hypothalamus orchestrates feeding. Science *341*, 1517–1521. https://doi.org/10.1126/science.1241812.
20. Nieh, E.H., Matthews, G.A., Allsop, S.A., Presbrey, K.N., Leppla, C.A., Wichmann, R., Neve, R., Wildes, C.P., and Tye, K.M. (2015). Decoding neural circuits that control compulsive sucrose seeking. Cell *160*, 528–541. https://doi.org/10.1016/j.cell.2015.01.003.
21. Schiffino, F.L., Siemian, J.N., Petrella, M., Laing, B.T., Sarsfield, S., Borja, C.B., Gajendiran, A., Zuccoli, M.L., and Aponte, Y. (2019). Activation of a lateral hypothalamic-ventral tegmental circuit gates motivation. PLoS One *14*, 0219522. https://doi.org/10.1371/journal.pone.0219522.
22. Siemian, J.N., Arenivar, M.A., Sarsfield, S., Borja, C.B., Russell, C.N., and Aponte, Y. (2021). Lateral hypothalamic LEPR neurons drive appetitive but not consummatory behaviors. Cell Rep. *36*, 109615. https://doi.org/10.1016/j.celrep.2021.109615.
23. Omrani, A., de Vrind, V.A., Lodder, B., Stoltenborg, I., Kooij, K., Wolterink-Donselaar, I.G., Luijendijk-Berg, M.C., Garner, K.M., van't Sant, L.J., Rozeboom, A., et al. (2021). Identification of novel neurocircuitry through which leptin targets multiple inputs to the dopamine system to reduce food reward seeking. Biol. Psychiatr. *90*, 843–852. https://doi.org/10.1016/j.biopsych.2021.02.017.
24. de Vrind, V.A.J., Rozeboom, A., Wolterink-Donselaar, I.G., Luijendijk-Berg, M.C.M., and Adan, R.A.H. (2019). Effects of GABA and leptin receptor-expressing neurons in the lateral hypothalamus on feeding, locomotion, and thermogenesis. Obesity *27*, 1123–1132. https://doi.org/10.1002/oby.22495.
25. Davis, J.F., Choi, D.L., Schurdak, J.D., Fitzgerald, M.F., Clegg, D.J., Lipton, J.W., Figlewicz, D.P., and Benoit, S.C. (2011). Leptin regulates energy balance and motivation through action at distinct neural circuits. Biol. Psychiatry *69*, 668–674. https://doi.org/10.1016/j.biopsych.2010.08.028.
26. Laque, A., Yu, S., Qualls-Creekmore, E., Gettys, S., Schwartzenburg, C., Bui, K., Rhodes, C., Berthoud, H.R., Morrison, C.D., Richards, B.K., and Munzberg, H. (2015). Leptin modulates nutrient reward via inhibitory galanin action on orexin neurons. Mol. Metab. *4*, 706–717. https://doi.org/10.1016/j.molmet.2015.07.002.
27. Brown, J.A., Wright, A., Bugescu, R., Christensen, L., Olson, D.P., and Leinninger, G.M. (2019). Distinct subsets of lateral hypothalamic neurotensin neurons are activated by leptin or dehydration. Sci. Rep. *9*, 1873. https://doi.org/10.1038/s41598-018-38143-9.
28. Kurt, G., Woodworth, H.L., Fowler, S., Bugescu, R., and Leinninger, G.M. (2019). Activation of lateral hypothalamic area neurotensin-expressing neurons promotes drinking. Neuropharmacology *154*, 13–21. https://doi.org/10.1016/j.neuropharm.2018.09.038.
29. Kurt, G., Kodur, N., Quiles, C.R., Reynolds, C., Eagle, A., Mayer, T., Brown, J., Makela, A., Bugescu, R., Seo, H.D., et al. (2022). Time to drink: activating lateral hypothalamic area neurotensin neurons promotes intake of fluid over food in a time-dependent manner. Physiol. Behav. *247*, 113707. https://doi.org/10.1016/j.physbeh.2022.113707.
30. Brown, J., Sagante, A., Mayer, T., Wright, A., Bugescu, R., Fuller, P.M., and Leinninger, G. (2018). Lateral hypothalamic area neurotensin neurons are required for control of orexin neurons and energy balance. Endocrinology *159*, 3158–3176. https://doi.org/10.1210/en.2018-00311.
31. Woodworth, H.L., Beekly, B.G., Batchelor, H.M., Bugescu, R., Perez-Bonilla, P., Schroeder, L.E., and Leinninger, G.M. (2017). Lateral hypothalamic neurotensin neurons orchestrate dual weight loss behaviors via distinct mechanisms. Cell Rep. *21*, 3116–3128. https://doi.org/10.1016/j.celrep.2017.11.068.
32. Tremblay, A., and Bellisle, F. (2015). Nutrients, satiety, and control of energy intake. Appl. Physiol. Nutr. Metab. *40*, 971–979. https://doi.org/10.1139/apnm-2014-0549.
33. Blundell, J., de Graaf, C., Hulshof, T., Jebb, S., Livingstone, B., Lluch, A., Mela, D., Salah, S., Schuring, E., Van Der Knaap, H., and Westerterp, M. (2010). Appetite control: methodological aspects of the evaluation of foods. Obes. Rev. *11*, 251–270. https://doi.org/10.1111/j.1467-789X.2010.00714.x.APPETITE.
34. Zhang, L.N., Mitchell, S.E., Hambly, C., Morgan, D.G., Clapham, J.C., and Speakman, J.R. (2012). Physiological and behavioral responses to intermittent starvation in C57BL/6J mice. Physiol. Behav. *105*, 376–387. https://doi.org/10.1016/j.physbeh.2011.08.035.
35. Lampe, J.W., Navarro, S.L., Hullar, M.A.J., and Shojaie, A. (2013). Inter-individual differences in response to dietary intervention: integrating omics platforms towards personalised dietary recommendations. Proc. Nutr. Soc. *72*, 207–218. https://doi.org/10.1017/S0029665113000025.
36. Campfield, L.A., Smith, F.J., Guisez, Y., Devos, R., and Burn, P. (1995). Recombinant mouse OB protein: evidence for a peripheral signal linking adiposity and central neural networks. Science *269*, 546–549. https://doi.org/10.1126/science.7624778.
37. Halaas, J.L., Gajiwala, K.S., Maffei, M., Cohen, S.L., Chait, B.T., Rabinowitz, D., Lallone, R.L., Burley, S.K., and Friedman, J.M. (1995).

Weight-reducing effects of the plasma protein encoded by the obese gene. Science *269*, 543–546. https://doi.org/10.1126/science.7624777.

38. Pelleymounter, M.A., Cullen, M.J., Baker, M.B., Hecht, R., Winters, D., Boone, T., and Collins, F. (1995). Effects of the obese gene product on body weight regulation in ob/ob mice. Science *269*, 540–543. https://doi.org/10.1126/science.7624776.

39. Friedman, J.M. (2019). Leptin and the endocrine control of energy balance. Nat. Metab. *1*, 754–764. https://doi.org/10.1038/s42255-019-0095-y.

40. Pan, W.W., and Myers, M.G. (2018). Leptin and the maintenance of elevated body weight. Nat. Rev. Neurosci. *19*, 95–105. https://doi.org/10.1038/nrn.2017.168.

41. Leinninger, G.M., Jo, Y.H., Leshan, R.L., Louis, G.W., Yang, H., Barrera, J.G., Wilson, H., Opland, D.M., Faouzi, M.A., Gong, Y., et al. (2009). Leptin acts via leptin receptor-expressing lateral hypothalamic neurons to modulate the mesolimbic dopamine system and suppress feeding. Cell Metab. *10*, 89–98. https://doi.org/10.1016/j.cmet.2009.06.011.

42. Wiltschko, A.B., Johnson, M.J., Iurilli, G., Peterson, R.E., Katon, J.M., Pashkovski, S.L., Abraira, V.E., Adams, R.P., and Datta, S.R. (2015). Mapping sub-second structure in mouse behavior. Neuron *88*, 1121–1135. https://doi.org/10.1016/j.neuron.2015.11.031.

43. Burnett, C.J., Li, C., Webber, E., Tsaousidou, E., Xue, S.Y., Brüning, J.C., and Krashes, M.J. (2016). Hunger-driven motivational state competition. Neuron *92*, 187–201. https://doi.org/10.1016/j.neuron.2016.08.032.

44. Leinninger, G.M., Opland, D.M., Jo, Y.H., Faouzi, M., Christensen, L., Cappellucci, L.A., Rhodes, C.J., Gnegy, M.E., Becker, J.B., Pothos, E.N., et al. (2011). Leptin action via neurotensin neurons controls orexin, the mesolimbic dopamine system and energy balance. Cell Metab. *14*, 313–323. https://doi.org/10.1016/j.cmet.2011.06.016.

45. Brown, J.A., Bugescu, R., Mayer, T.A., Gata-Garcia, A., Kurt, G., Woodworth, H.L., and Leinninger, G.M. (2017). Loss of action via neurotensin-leptin receptor neurons disrupts leptin and ghrelin-mediated control of energy balance. Endocrinology *158*, 1271–1288. https://doi.org/10.1210/en.2017-00122.

46. Mickelsen, L.E., Bolisetty, M., Chimileski, B.R., Fujita, A., Beltrami, E.J., Costanzo, J.T., Naparstek, J.R., Robson, P., and Jackson, A.C. (2019). Single-cell transcriptomic analysis of the lateral hypothalamic area reveals molecularly distinct populations of inhibitory and excitatory neurons. Nat. Neurosci. *22*, 642–656. https://doi.org/10.1038/s41593-019-0349-8.

47. Flak, J.N., and Myers, M.G. (2016). Minireview: CNS mechanisms of leptin action. Mol. Endocrinol. *30*, 3–12. https://doi.org/10.1210/me.2015-1232.

48. Chrysafi, P., Perakakis, N., Farr, O.M., Stefanakis, K., Peradze, N., Sala-Vila, A., and Mantzoros, C.S. (2020). Leptin alters energy intake and fat mass but not energy expenditure in lean subjects. Nat. Commun. *11*, 5145. https://doi.org/10.1038/s41467-020-18885-9.

49. Cohen, P., Zhao, C., Cai, X., Montez, J.M., Rohani, S.C., Feinstein, P., Mombaerts, P., and Friedman, J.M. (2001). Selective deletion of leptin receptor in neurons leads to obesity. J. Clin. Invest. *108*, 1113–1121. https://doi.org/10.1172/JCI200113914.

50. Kowalski, T.J., Liu, S.-M., Leibel, R.L., and Chua, S.C. (2001). Transgenic complementation of leptin-receptor deficiency. I. Rescue of the obesity/diabetes phenotype of LEPR-null mice expressing a LEPR-B transgene. Diabetes *50*, 425–435. https://doi.org/10.2337/diabetes.50.2.425.

51. Aponte, Y., Atasoy, D., and Sternson, S.M. (2011). AGRP neurons are sufficient to orchestrate feeding behavior rapidly and without training. Nat. Neurosci. *14*, 351–355. https://doi.org/10.1038/nn.2739.

52. Rogan, S.C., Koda, S., Ye, C., Krashes, M.J., Adams, A.C., Cusher, D.S., Maratos-Flier, E., Roth, B.L., Lowell, B.B., Maratos-flier, E., et al. (2011). Rapid, reversible activation of AgRP neurons drives feeding behavior in mice. J. Clin. Invest. *121*, 1424–1428. https://doi.org/10.1172/JCI46229.1424.

53. Meister, B. (2007). Neurotransmitters in key neurons of the hypothalamus that regulate feeding behavior and body weight. Physiol. Behav. *92*, 263–271. https://doi.org/10.1016/j.physbeh.2007.05.021.

54. Jennings, J.H., Kim, C.K., Marshel, J.H., Raffiee, M., Ye, L., Quirin, S., Pak, S., Ramakrishnan, C., and Deisseroth, K. (2019). Interacting neural ensembles in orbitofrontal cortex for social and feeding behaviour. Nature *565*, 645–649. https://doi.org/10.1038/s41586-018-0866-8.

55. Fu, O., Iwai, Y., Narukawa, M., Ishikawa, A.W., Ishii, K.K., Murata, K., Yoshimura, Y., Touhara, K., Misaka, T., Minokoshi, Y., and Nakajima, K.I. (2019). Hypothalamic neuronal circuits regulating hunger-induced taste modification. Nat. Commun. *10*, 4560. https://doi.org/10.1038/s41467-019-12478-x.

56. Takahashi, K.A., and Cone, R.D. (2005). Fasting induces a large, leptin-dependent increase in the intrinsic action potential frequency of orexigenic arcuate nucleus neuropeptide Y/Agouti-related protein neurons. Endocrinology *146*, 1043–1047. https://doi.org/10.1210/en.2004-1397.

57. Perry, R.J., Resch, J.M., Douglass, A.M., Madara, J.C., Rabin-Court, A., Kucukdereli, H., Wu, C., Song, J.D., Lowell, B.B., and Shulman, G.I. (2019). Leptin's hunger-suppressing effects are mediated by the hypothalamic–pituitary–adrenocortical axis in rodents. Proc. Natl. Acad. Sci. USA *116*, 13670–13679. https://doi.org/10.1073/pnas.1901795116.

58. Pedroso, J.A.B., Silveira, M.A., Lima, L.B., Furigo, I.C., Zampieri, T.T., Ramos-Lobo, A.M., Buonfiglio, D.C., Teixeira, P.D.S., Frazão, R., and Donato, J. (2016). Changes in leptin signaling by SOCS3 modulate fasting-induced hyperphagia and weight regain in mice. Endocrinology *157*, 3901–3914. https://doi.org/10.1210/en.2016-1038.

59. van Baak, M.A., and Mariman, E.C.M. (2019). Mechanisms of weight regain after weight loss — the role of adipose tissue. Nat. Rev. Endocrinol. *15*, 274–287. https://doi.org/10.1038/s41574-018-0148-4.

60. Montemurro, D.G., and Stevenson, J.A. (1957). Adipsia produced by hypothalamic lesions in the rat. Can. J. Biochem. Physiol. *35*, 31–37. https://doi.org/10.1139/y57-005.

61. Berthoud, H.R., and Münzberg, H. (2011). The lateral hypothalamus as integrator of metabolic and environmental needs: from electrical self-stimulation to optogenetics. Physiol. Behav. *104*, 29–39. https://doi.org/10.1016/j.physbeh.2011.04.051.

62. Opland, D., Sutton, A., Woodworth, H., Brown, J., Bugescu, R., Garcia, A., Christensen, L., Rhodes, C., Myers, M., and Leinninger, G. (2013). Loss of neurotensin receptor-1 disrupts the control of the mesolimbic dopamine system by leptin and promotes hedonic feeding and obesity. Mol. Metab. *2*, 423–434. https://doi.org/10.1016/j.molmet.2013.07.008.

63. Gropp, E., Shanabrough, M., Borok, E., Xu, A.W., Janoschek, R., Buch, T., Plum, L., Balthasar, N., Hampel, B., Waisman, A., et al. (2005). Agouti-related peptide-expressing neurons are mandatory for feeding. Nat. Neurosci. *8*, 1289–1291. https://doi.org/10.1038/nn1548.

64. Ahima, R.S., Prabakaran, D., Mantzoros, C., Qu, D., Lowell, B., Maratos-Flier, E., and Flier, J.S. (1996). Role of leptin in the neuroendocrine response to fasting. Nature *382*, 250–252. https://doi.org/10.1038/382250a0.

65. Wade, G.N., Lempicki, R.L., Panicker, A.K., Frisbee, R.M., and Blaustein, J.D. (1997). Leptin facilitates and inhibits sexual behavior in female hamsters. Am. J. Physiol. *272*, R1354–R1358. https://doi.org/10.1152/ajpregu.1997.272.4.R1354.

66. Louis, G.W., Leinninger, G.M., Rhodes, C.J., and Myers, M.G. (2010). Direct innervation and modulation of orexin neurons by lateral hypothalamic LepRb neurons. J. Neurosci. *30*, 11278–11287. https://doi.org/10.1523/JNEUROSCI.1340-10.2010.

67. Giardino, W.J., Eban-Rothschild, A., Christoffel, D.J., Li, S.B., Malenka, R.C., and de Lecea, L. (2018). Parallel circuits from the bed nuclei of stria terminalis to the lateral hypothalamus drive opposing emotional states. Nat. Neurosci. *21*, 1084–1095. https://doi.org/10.1038/s41593-018-0198-x.

68. Berridge, C.W., España, R.A., and Vittoz, N.M. (2010). Hypocretin/orexin in arousal and stress. Brain Res. *1314*, 91–102. https://doi.org/10.1016/j.brainres.2009.09.019.

69. Bonnavion, P., Jackson, A.C., Carter, M.E., and De Lecea, L. (2015). Antagonistic interplay between hypocretin and leptin in the lateral

hypothalamus regulates stress responses. Nat. Commun. *6*, 6266. https://doi.org/10.1038/ncomms7266.

70. Ranjan, S., and Nasser, J.A. (2015). Nutritional status of individuals with autism spectrum disorders: do we know enough? Adv. Nutr. *6*, 397–407. https://doi.org/10.3945/an.114.007914.
71. Kaye, W.H., Bulik, C.M., Thornton, L., Barbarich, N., Masters, K., Barbarich, N., and Masters, K. (2004). Comorbidity of anxiety disorders with anorexia and bulimia nervosa. Am. J. Psychiatry *161*, 2215–2221.
72. Xu, S., Yang, H., Menon, V., Lemire, A.L., Wang, L., Henry, F.E., Turaga, S.C., and Sternson, S.M. (2020). Behavioral state coding by molecularly defined paraventricular hypothalamic cell type ensembles. Science *370*, eabb2494. https://doi.org/10.1126/science.abb2494.
73. Leshan, R.L., Björnholm, M., Münzberg, H., and Myers, M.G. (2006). Leptin receptor signaling and action in the central nervous system. Obesity *14*, 208S–212S. https://doi.org/10.1038/oby.2006.310.
74. Giovannucci, A., Friedrich, J., Gunn, P., Kalfon, J., Brown, B.L., Koay, S.A., Taxidis, J., Najafi, F., Gauthier, J.L., Zhou, P., et al. (2019). Caiman an open source tool for scalable calcium imaging data analysis. eLife *8*, e38173. https://doi.org/10.7554/eLife.38173.
75. Bender, F., Gorbati, M., Cadavieco, M.C., Denisova, N., Gao, X., Holman, C., Korotkova, T., and Ponomarenko, A. (2015). Theta oscillations regulate the speed of locomotion via a hippocampus to lateral septum pathway. Nat. Commun. *6*, 8521. https://doi.org/10.1038/ncomms9521.
76. Vogelstein, J.T., Packer, A.M., Machado, T.A., Sippy, T., Babadi, B., Yuste, R., and Paninski, L. (2010). Fast nonnegative deconvolution for spike train inference from population calcium imaging. J. Neurophysiol. *104*, 3691–3704. https://doi.org/10.1152/jn.01073.2009.
77. Pnevmatikakis, E.A., Soudry, D., Gao, Y., Machado, T.A., Merel, J., Pfau, D., Reardon, T., Mu, Y., Lacefield, C., Yang, W., et al. (2016). Simultaneous denoising, deconvolution, and demixing of calcium imaging data. Neuron *89*, 285–299. https://doi.org/10.1016/j.neuron.2015.11.037.
78. Ung, R.L. (2019). Neural Dynamic Adaptation of Extended Amygdala to Stress and Anxiety (Univ. North Carolina Chapel Hill). https://doi.org/10.17615/bs3p-7p36.

Please cite this article in press as: Petzold et al., Complementary lateral hypothalamic populations resist hunger pressure to balance nutritional and social needs, Cell Metabolism (2023), https://doi.org/10.1016/j.cmet.2023.02.008

STAR★METHODS

KEY RESOURCES TABLE

REAGENT or RESOURCE	SOURCE	IDENTIFIER
Bacterial and virus strains		
AAV-DJ-EF1a-DIO-GCaMP6m	UNC Vector Core	N/A
AAV-EF1a-DIO-hChR2(H134R)-EYFP	Addgene	Cat#35507; RRID: Addgene_35507
AAV-EF1a-DIO-EYFP-WPRE-pA	Addgene	Cat#27056; RRID: Addgene_27056
AAV8-hSyn-DIO-hM3D(Gq)-mCherry	Addgene	Cat#44361; RRID: Addgene_44361
AAV8-hSyn-DIO-mCherry	Addgene	Cat#50459; RRID: Addgene_50459
Chemicals, peptides, and recombinant proteins		
Clozapine-N-Oxide (CNO)	HelloBio	Cat#HB1807
Leptin	Sigma/Merck	Cat#L3772
Experimental models: Organisms/strains		
Mouse: $LepR^{Cre}$	JAX[73]	Cat#032457; RRID: IMSR_JAX:032,457
Mouse: Nts^{Cre}	JAX[44]	Cat#017525; RRID: IMSR_JAX:017,525
Mouse: C57BL/6	JAX	Cat#000664; RRID: IMSR_JAX:000,664
Software and algorithms		
R v4.1.2	R Foundation	N/A
Python v2.7	Python Software Foundation	N/A
ANY-maze behavioral tracking software v6.33	Stoelting	Cat#60000
Adobe Premiere	Adobe	N/A
FiJi	NIH	N/A
nVista HD	Inscopix	N/A
CaImAn	[74]	N/A
MoSeq v1	[42]	N/A
Other		
Dustless, normal chow precision pellets (20 mg)	Bio-Serv	Cat#F0071
nVista Imaging System for Rodents	Inscopix	Cat#1000-002671
GRIN lens probe, 0.6 x 7.3 mm	Inscopix	Cat#1050-002208
Baseplate	Inscopix	Cat#1050-002192
Pro-View kit	Inscopix	Cat#1050-002310
Miniscope gripper	Inscopix	Cat#1050-002199
AMi-2 optogenetics interface	Stoelting	Cat#60060
LRS-0473 DPSS Laser System	Laserglow Technologies	Cat#R471005FX

RESOURCE AVAILABILITY

Lead contact

Further information and requests for resources and reagents should be directed to and will be fulfilled by the lead contact, Tatiana Korotkova (tatiana.korotkova@uk-koeln.de).

Materials availability

This study did not generate new unique reagents.

Data and code availability

- Data used for statistical analysis is supplied in a separate file (Data S1).
- Original code used to analyze the data is supplied in a separate file (Methods S1).
- Any additional information required to analyze the data reported in this paper is available from the corresponding author upon reasonable request.

Please cite this article in press as: Petzold et al., Complementary lateral hypothalamic populations resist hunger pressure to balance nutritional and social needs, Cell Metabolism (2023), https://doi.org/10.1016/j.cmet.2023.02.008

EXPERIMENTAL MODEL AND SUBJECT DETAILS

Adult LepR-Cre (JAX #032457),[73] Nts-Cre (JAX #017525),[44] and C57BL/6 mice (JAX #000664) were used in this study (The Jackson Laboratory, Bar Harbor, USA). Both Cre lines were backcrossed to the C57BL6/J strain. All experimental procedures were performed in accordance with national and international guidelines (ARRIVE) and approved by the local health authority (LANUV). Animals were housed in groups in the animal facility under standard conditions at a room temperature between 20 and 24°C and on a reversed 12 h light/dark cycle (lights off at 9 a.m.). Animals were provided with standard chow (V1554-703, Ssniff, Soest, Germany) and water *ad libitum*, unless placed on a restriction schedule. Animals of both sexes were used, and were 12–16 weeks of age at the start of the experiment.

METHOD DETAILS

Surgical procedures

Viral injections

Injections were performed as described previously.[5,75] Preceding surgeries, buprenorphin (0.1 mg/kg, Buprenovet sine, Bayer, Leverkusen, Germany) was administered subcutaneously. Animals were anesthetized with isoflurane and mounted in a stereotactic frame (Kopf Instruments, Tujunga, CA, USA). Anesthesia was maintained with isoflurane. Body temperature was continuously monitored using a rectal thermometer while animals were kept on top of a heating pad (Stoelting, Wood Dale, IL, USA) throughout the surgery to avoid hypothermia. Eyes were moisturized with ophthalmic ointment (Bepanthen, Bayer, Leverkusen, Germany) to avoid drying. After cutting the fur on top of the head, lidocaine was applied to the skin and a small incision was made to expose the skull. Small craniotomies were drilled dorsal to the injection sites and cleaned with ice-cold PBS. Virus suspension (~250 nL per level) was infused with a 30-gauge needle (Hamilton, Reno, NV, USA) in a stereotactic mounted nanopump (Hugo Sachs Elektronik - Harvard Apparatus, Freiburg im Breisgau, Germany) at a rate of 150 nL/min. After infusion, the needle was kept at the injection site for 10 min, in order to allow sufficient time for viral spread, and then slowly removed before the incision was sutured and treated with lidocaine cream (EMLA, Aspen Germany GmbH, Munich). Animals were treated with Carprofen (5 mg/kg, Rimadyl, Zoetis, Berlin, Germany) for 3 days and recovered in the home cage until sufficient virus expression was obtained. Viral constructs were provided by the UNC Gene Therapy Center Vector Core (University of North Carolina at Chapel Hill, Chapel Hill, NC, USA) or Addgene (Watertown, MA, USA). For Ca^{2+} imaging, AAV-DJ-EF1a-DIO-GCaMP6m (UNC; 5 x 10^{12} GC/mL) was used. For optogenetic experiments, AAV-EF1a-DIO-hChR2(H134R)-EYFP was used for optogenetic excitation and AAV-EF1a-DIO-EYFP-WPRE-pA (Addgene 27,056-AAV2; 1 x 10^{12} GC/mL) was used in the control group. For chemogenetic experiments, AAV8-hSyn-DIO-hM3D(Gq)-mCherry (Addgene 44,361-AAV8; 2.5 x 10^{13} GC/mL) was used for chemogenetic excitation and AAV8-hSyn-DIO-mCherry (50,459-AAV8; 2.1 x 10^{13} GC/mL) was used in the control group. The LH was targeted bilaterally at anterior-posterior (AP) 1.3, lateral (L) +0.9 and ventral (V) 5.2, 5.4 mm from the bregma.[75]

Implantation of optic fibers

Optic fibers were manufactured on site from 100 μm-diameter optical fibers (0.22 numerical aperture (NA), Thorlabs, Newton, NJ, USA) and ceramic fiber optic ferrules (Thorlabs, Newton, NJ, USA). Craniotomies were drilled anterior and posterior to injection sites to accommodate two screws (Kopf Instruments, Tujunga, CA, USA) to stabilize the implant. Following virus injection, optic fibers were implanted into the LH at AP 1.3, L + 1.0 and V 4.9 mm through the craniotomies used for injection, and secured to the skull using dental cement (Metabond, Parkell, Edgewood, NY, USA) around the fibers and screws, which was then covered with blackened glue (Loctite, Henkel, Dusseldorf, Germany).

GRIN lens implantation

Straight cuffed GRIN lenses (0.5 NA, 3/2 pitch, 0.6 × 7.3 mm; Inscopix, Palo Alto, CA, USA) were used. Craniotomies were drilled anterior and posterior to the implantation site to accommodate two screws (Kopf Instruments, Tujunga, CA, USA) to stabilize the implant. A craniotomy was drilled with a trephine bit (1.8 mm diameter tip; Fine Science Tools, Foster City, CA, USA) above the LH, in order to accommodate the lens at around AP 1.3 and L −1 mm from the bregma under continuous application of ice-cold PBS. Following virus injection, the lens was inserted into a stereotactic mounted holder (Pro-View kit; Inscopix, Palo Alto, CA, USA) and slowly lowered at a rate of 100 μm/min from V 0 to 2.5 mm and at a rate of 50 μm/min from V 2.5 to around 5.0 mm from the bregma. The skull was thoroughly dried and the lens was secured to the skull with Metabond (Parkell, Edgewood, NY, USA). The lens was protected with Parafilm, which was secured to the cuff of the lens by a silicone elastomer (KWIK CAST, WPI LLC, Hertfordshire, UK). The incised skin was treated with lidocaine cream (EMLA, Aspen Germany GmbH, Munich). Animals were treated with Carprofen as described above and recovered in the home cage for at least 2 weeks.

To support the microendoscope on the animal's head, a baseplate (Inscopix, Palo Alto, CA, USA) was secured to the skull. To determine the optimal position of the baseplate, the animal was anesthetized and mounted into the stereotaxic frame. The protective silicone mount was carefully removed with forceps. The baseplate was secured to the microendoscope (2 g; 650 × 900 μm FOV; single-channel epifluorescence: 475 nm blue LED; Inscopix, Palo Alto, CA, USA) with a fixation screw and mounted onto the stereotaxic frame with an adjustable gripper (Inscopix, Palo Alto, CA, USA). The microendoscope was lowered toward the lens until cells came into focus. In this position, the baseplate was secured to the skull with Metabond (Parkell, Edgewood, NY, USA). After removal of the microendoscope, the baseplate was sealed with a protective cover (Inscopix, Palo Alto, CA, USA).

Deep brain single-cell imaging

Ca^{2+} imaging in freely behaving mice

To attach the microendoscope, the animal was gently fixated by hand, the protective cover removed and the microendoscope secured to the baseplate with a fixation screw. Animals acclimated in their home cages for 5 min before the start of the experiment.

Data acquisition and processing

Greyscale tiff images were acquired using the nVista HD 2 software (Inscopix, Palo Alto, CA) at 10 frames/s with an average exposure time of 100 s. Video streams from Ca^{2+} and behavioral imaging were triggered via TTL pulses delivered by an AMi interface (Stoelting, Wood Dale, IL, USA) and controlled by ANY-maze (Stoelting, Wood Dale, IL, USA). All Ca^{2+} image processing was performed using the CaImAn library for Python (https://github.com/flatironinstitute/CaImAn)[74] and custom Python scripts to run Ca^{2+} trace extraction automatically in batch mode. Recordings were cropped to remove empty parts of the FOV and artifacts, such as the rim of the lens, and spatially downsampled in the X and Y dimensions by a factor of two. All frames collected over the course of a session were concatenated and registered to each other using a rigid registration method. Individual Ca^{2+} traces and spatial filters were extracted from the registered recordings using CNMF-E.[74] To ensure high quality segmentation, all extracted components were manually refined to exclude components with traces that contained motion artifacts, high noise levels or components with ROIs that lacked a round, soma-like shape. Ca^{2+} traces were denoised and deconvolved using sparse non-negative deconvolution.[76,77] Individual Ca^{2+} traces were z-scored across all trials of a single day and averaged over 1 s bins.

Longitudinal registration across experimental sessions

Motion corrected, refined components were registered across experimental days using the *multi_session* function in CaImAn.[74]

Optogenetic stimulation and data acquisition

A 3-m fiberoptic patch cord with protective tubing (25 μm diameter, 0.1 NA; Thorlabs, Newton, NJ, USA) was connected to the optic fibers via a ferrule and to a 473 nm diode-pumped solid-state laser (R471005FX, Laserglow Technologies, Toronto, Canada) with an FC/PC adapter. Laser output was controlled via TTL pulses generated by an AMi optogenetic interface and controlled by a stimulation protocol run by the ANY-maze software (v6.33, Stoelting, Wood Dale, IL, USA). Stimulation was delivered unilaterally and consisted of 5 ms blue (473 nm) light pulses delivered at 20 Hz with a light power output of ~20 mW measured at the tip of the patch cord with a power meter (PM100D, Thorlabs, Newton, NJ, USA). ANY-maze (Stoelting, Wood Dale, IL, USA) was also used to acquire a video stream (30 Hz frame rate, DMK22BUC03, Imaging Source Europe GmbH, Bremen, Germany) and to track animals throughout the experiment.

Chemogenetic stimulation and data acquisition

Mice expressing either hM3D(Gq)-mCherry or mCherry were injected with CNO (1 mg/kg i.p., Hellobio, Bristol, UK) 30 min prior to the start of experiments. Recordings of 20 min per mouse were taken with a depth camera (30 Hz frame rate; Kinect for Windows v.2, Microsoft, Redmond, WA, USA) positioned 65 cm above the floor of the arena. Using custom Python scripts adapted from MoSeq v.1[42] by Randall Ung,[78] depth images were saved in hdf5 format, together with frame timestamps, a region of interest (ROI) polygon delimiting the boundaries of the arena and 2D images to inspect the behavioral syllables after analyses. After acquisition, hdf5 depth images were converted into raw binary format (16-bit signed integers) for further analysis. We also acquired a monochromatic video stream (30 Hz frame rate, DMK22BUC03, Imaging Source Europe GmbH, Bremen, Germany) for processing with conventional behavior software (ANY-maze, v6.33, Stoelting, Wood Dale, IL, USA).

Behavioral assays

All behavioral experiments were standardized and conducted in the active dark phase (starting at the beginning of the dark cycle). In all behavioral assays, animals were recorded using a monochrome USB camera (30 Hz frame rate, DMK22BUC03, Imaging Source, Bremen, Germany) positioned above the arena and controlled by a recording schedule run by ANY-maze (v6.33, Stoelting, Wood Dale, IL, USA). ANY-maze was also used to acquire the video stream and to track animals throughout the experiment.

Free access feeding task for Ca^{2+} imaging and optogenetic experiments

Prior to food restriction, we predetermined the average body weight and the amount of food individual animals consumed each day and restricted their normal daily intake for 5 days such that animals lost weight continuously but no more than 20% of their initial body weight. Animals were habituated to the plexiglass enclosure (WDH: 50 × 30 × 40 cm) containing food (20 mg dustless precision pellets, #F0071, Bio-serv, Flemington, NJ, USA) and water trays as well as a tray containing objects (paper clips) and an empty mesh.

For Ca^{2+} imaging experiments, animals were recorded in the free access enclosure before food restriction and after 1 and 5 days of food restriction, thus covering the sated state, as well as acute and chronic hunger states. Animals were allowed to freely explore the enclosure. After 10 min, a female conspecific was placed behind the mesh for another 10 min of recording. Besides recording Ca^{2+} activity, we also measured the amount of food animals consumed in each 10-min block.

For optogenetic experiments, mice expressing either hChR2-EYFP or EYFP were placed in the free access enclosure containing food, water, objects and a female conspecific behind a mesh and freely explored the arena for 10 min. Blue light (473 nm) was delivered in 5 ms pulses at 20 Hz.

Feeding rebound and weight categories

Animals were grouped according to their food intake during the daily session in the free access enclosure. Animals that consumed more than the average amount were classified as "voracious feeders" and animals that consumed less than the average amount

Please cite this article in press as: Petzold et al., Complementary lateral hypothalamic populations resist hunger pressure to balance nutritional and social needs, Cell Metabolism (2023), https://doi.org/10.1016/j.cmet.2023.02.008

were classified as "moderate feeders". For some analyses, we compared the Ca^{2+} activity of $LepR^{LH}$ neurons in fat animals to the Ca^{2+} activity of $LepR^{LH}$ neurons in lean animals. For this purpose, we split animals into fat/lean weight categories: "fat" animals weighted more than the daily average weight across all animals, "lean" animals weighted less than average.

Comparison of food and water deprivation

To compare the effect of hunger and thirst on neural activity, we predetermined the initial body weight and food intake in the free access enclosure in the sated state when animals had access to food and water *ad libitum*. Animals were then deprived of food for 22 h and recorded in the free access enclosure. Animals were given access to food and water for 2 h immediately after the test, and then deprived of water for 22 h until they were recorded in the free access enclosure. Each Ca^{2+} recording lasted 20 min. Animals were given *ad libitum* access to food and water after the test.

Free access feeding task for chemogenetic experiments

For a detailed assessment of behavioral dynamics using MoSeq,[42] chemogenetic activation was combined with a depth camera recording. As a standard free access enclosure was incompatible with the depth camera recordings, we adapted the enclosure (WDH: 20 × 30 × 40 cm, opaque polyethylene sanded to reduce reflections) to contain cups of water, 10 mg food pellets and an object (piece of Lego). Animals were injected with CNO (1 mg/kg, i.p., Hellobio, Bristol, UK) 30 min before the start of the experiment when they were placed in the arena and then allowed to freely explore the enclosure for 20 min.

Food and water intake measurement upon chemogenetic stimulation

Mice expressing either hM3D(Gq)-mCherry or mCherry were injected with CNO (1 mg/kg, i.p., Hellobio, Bristol, UK) in their home cage at the start of the dark phase. Water and food (normal chow) intake were measured each hour for 7 consecutive hours after injection.

Food intake measurement during optogenetic stimulation

We tested the effects on acute and chronic hunger in separate experiments. In the first set of experiments, we tested animals in the free access enclosure in the sated state and following food deprivation. In the second set of experiments, we tested animals in the sated state and after 5 days of food restriction performed as described above. Food intake was measured for 10 min and blue light (473 nm) was delivered in 5 ms pulses at 20 Hz. In Figure 3H, total intake of experimental animals was normalized by the average total intake of the control group.

Water intake measurement during optogenetic stimulation

To measure water intake during optogenetic stimulation, animals were water deprived for 22 h before accessing a tube (Falcon) filled with 10 mL water and equipped with a spout in the home cage. Tubes were weighed before and after the test to determine the amount of water consumed during the test. Water intake was measured for 30 min and blue light (473 nm) was delivered in 5 ms pulses at 20 Hz.

Social interaction task in Ca^{2+} imaging and optogenetic experiments

For consistent presentation of social stimuli, a three chamber arena (WDH: 50 × 30 × 40 cm) made of Plexiglas containing two social and one center zone was used. Each social location contained a metal mesh (WDH: 8 × 8 × 7 cm). Animals were introduced into the arena to explore the social locations with an empty mesh each. First, a conspecific was placed under one mesh and the animals were allowed to freely explore the empty and occupied mesh for 5 min. Then, a conspecific was placed under the empty mesh and the animal was allowed to freely explore both conspecifics for another 5 min. Blue light (473 nm) was delivered in 5 ms pulses at 20 Hz. We conducted this experiment once with male and once with female conspecifics separated by at least 24 h. For Ca^{2+} imaging experiments, we extended the test duration to 20 min to allow for sufficient data collection.

Social interaction task in chemogenetic experiments

We adapted the social task to be compatible with depth camera recordings for MoSeq analysis, i.e. modified the arena (WDH: 45 × 25 × 40 cm, opaque polyethylene) and extended the trial duration. Animals were injected with CNO (1 mg/kg, i.p., Hellobio, Bristol, UK) 30 min prior to the start of the experiment when they were introduced into the arena to freely explore a female conspecific under a metal mesh (WDH: 8 × 8 × 7 cm) on one side and a mesh with object on the other side. After 20 min, the object in the mesh was replaced by another female conspecific and animals were allowed to explore both occupied social zones for 20 min.

Pharmacological assays

All pharmacological experiments were conducted in the active dark phase.

Ca^{2+} imaging in freely behaving mice following drug injection

Ca^{2+} imaging was performed in the homecage. After attachment of the microendoscope (nVista2.0, Inscopix, Palo Alto, CA), animals were given 5 min to acclimatize to the microendoscope. Ca^{2+} imaging was performed for 5 min, 25 min after i.p. injection of PBS (Sigma/Merck, Darmstadt, Germany) or leptin (5 mg/kg; Sigma/Merck, Darmstadt, Germany).

Food and social seeking behavior following drug injection

For food intake measurements, acutely food-deprived animals were i.p. injected with PBS (Sigma/Merck, Darmstadt, Germany) or leptin (5 mg/kg; Sigma/Merck, Darmstadt, Germany) and returned to their homecage. Animals were given access to 20 mg precision pellets for 5 min starting at 25 min and 115 min after injection to record food intake at these timepoints. For social behavior experiments, acutely food-deprived male mice were i.p. injected with PBS and leptin and returned to their homecage. 120 min following injection, animals were introduced to the free-access enclosure containing food, water, a female conspecific, and an object for 10 min and the spontaneous behavior was recorded using automated video tracking.

Histology

All animals used in this study were terminally anesthetized and transcardially perfused shortly after the last test. Brains were dissected, cryoprotected in 30% sucrose and cryosectioned coronally. Relevant brain slices of each animal were imaged with a fluorescence widefield microscope (ZEISS Axio Imager 2, Zeiss, Leverkusen, Germany). Location and spread of the virus transduction were validated using a standardized atlas of the mouse brain (Paxinos & Franklin *Academic Press* 2001). Similarly, relevant brain slices were imaged with a confocal microscope (Leica SP8, Leica Camera AG, Wetzlar, Germany) to validate the position of optic fibers and lens probes.

Behavioral scoring

Animal position was tracked automatically throughout each experiment using ANY-maze (v6.33, Stoelting, Wood Dale, IL, USA). Behavioral enclosures were virtually divided into zones according to the respective stimulus locations, and the occupation of animals in zones was automatically detected through automated tracking using ANY-maze. Ethograms were obtained by standardized frame-by-frame scoring of feeding- and drinking-related behaviors using Adobe Premiere (Adobe, San Jose, CA, USA).

QUANTIFICATION AND STATISTICAL ANALYSIS

Animals of the same litter were randomly assigned to experimental groups. Injection sites and viral expression as well as placement of optic fibers or lens probes were confirmed for all animals. Mice with incorrect injection or implantation sites were excluded from data analysis. No data points were excluded from further analysis. All replicates constitute biological replicates.

Data analysis

Identification of stimulus-responsive cells

To identify cells that were significantly modulated when the animal occupied a stimulus location, the Ca^{2+} signal as well as velocity were binned (1 s bins) across the session and occupation of each stimulus zone was indicated with ones when it occurred. To fit the Ca^{2+} signal of individual cells, we applied a linear model (*stats* package, R). For the free access feeding task without a conspecific, the following predictors were used: occupation of a stimulus location (center zone; food, water or object location) and velocity. For the free access feeding task with a conspecific, the ''social location'' was added as a predictor. For the social access task, the following predictors were used: occupation of a stimulus location (the familiar female or male conspecific and the novel female or male conspecific), the center zone, and velocity. If the independent variables (predictors) of the linear model fitted to the activity of a cell were significant ($p < 0.05$), the cell was classified as ''modulated'' by the significant predictor, and ''non-responsive'' if not ($p > 0.05$). For significant predictors, positive regression coefficients defined ''excited'' cells, and negative regression coefficients defined ''inhibited'' cells, e.g. ''food-excited'' or ''food-inhibited'' cells. The Benjamini-Hochberg procedure was used to correct for multiple comparisons.

Identification of consecutive responses to stimulus

To identify cells that systematically changed their response over the course of a daily session, we averaged the Ca^{2+} signal for each visit to a stimulus location and applied a linear model (*stats* package, R) using the sequence of the first 8 visits as a predictor. Among neurons exhibiting a significant change of the Ca^{2+} signal across visits, we defined sensitizing neurons as neurons that significantly increased their response over time, i.e. excitatory neurons showing increase in Ca^{2+} signal or inhibitory neurons showing decrease in Ca^{2+} signal. Desensitizing neurons were defined as neurons that decreased their response over time, i.e. excitatory neurons showing decrease in Ca^{2+} signal or inhibitory neurons showing increase in Ca^{2+} signal.

Response dynamics during stimulus detection

For each cell, we used the pre-entry epoch in a 3 s-window before entry and the post-entry epoch in a 5 s-window after entry of the stimulus location. We applied a generalized additive model with penalized thin-plate regression splines (*mgcv* package, R) over Ca^{2+} signals across time points per epoch. As we observed rapid changes in Ca^{2+} signal upon entry of the water location, we quantified Ca^{2+} signals in balanced time windows of 3 s before and after entry of water or food location.

Behavioral motion segmentation (MoSeq)

Data analyses were executed in a virtual environment with Debian GNU/Linux 8, from a Linux (Ubuntu 16.94.3 LTS) compute cluster. Behavior was classified using MoSeq v.1.[42] Briefly, the depth mouse images were cropped along the arena boundaries, extracted from the arena background, parallax corrected and oriented along the spine axis. Time-series data were subjected to wavelet transformation and dimensionally compressed using PCA. To classify the behavioral syllables, an autoregressive hidden Markov model was applied to the first 10 principal components, taking into account differences in pose dynamics, duration distribution and transition distribution. A template matching procedure ensured that only repeated PC trajectories (i.e. meaningful ones) were selected as syllables. One of the model parameters, the self-transition bias kappa, was set to match the median syllable duration with the median approximate changepoint of each dataset identified using a filtered derivative algorithm (usually $\kappa = 5$ or $\kappa = 6$). Statistical differences in behavioral syllable proportions were evaluated by performing z-tests on bootstrap samples (calculated over the data of individual mice) with a Benjamini-Hochberg correction (false discovery rate = 0.1) for multiple comparisons. To qualitatively verify and define behavioral syllables, we manually assessed visualizations of each syllable on the basis of the 2D recordings.

Please cite this article in press as: Petzold et al., Complementary lateral hypothalamic populations resist hunger pressure to balance nutritional and social needs, Cell Metabolism (2023), https://doi.org/10.1016/j.cmet.2023.02.008

Relative behavioral stimulus preference

We calculated the relative preference for the three main innate rewards used in this study (food, water, conspecific) across need states (sated, hunger, thirst) during optogenetic stimulation by normalizing the time spent exploring each of these stimuli to the total amount of time spent exploring and then applied 2D kernel density estimation (*MASS* package, R) to obtain the density along the three dimensions.

Functional overlap of neural populations

To assess the overlap of stimulus-elicited responses between Nts^{LH} and $LepR^{LH}$ neurons, we estimated the kernel density of stimulus-elicited responses per population (*stats* package, R) and assessed the proportion of cells with overlapping responses between both populations (*overlap* package, R). If the distribution of stimulus-elicited responses across populations was multimodal ($p < 0.05$, excess mass test, *multimode* package, R), we estimated the location of modes using a non-parametric approach (locmodes function, *multimode* package, R).

Statistical analysis

Statistical tests were applied according to experimental design and data structure. Data, except for scatter and proportion plots, are presented as mean ± SEM. No statistical methods were used to predetermine sample sizes as they were chosen based on those reported in similar previous studies. Information on applied tests, sample size and test result is reported for each panel individually in the legend. We applied the Shapiro-Wilk test to determine normality of distribution. Depending on the normality of distribution, comparisons between two groups were performed using Student's *t* test or Mann-Whitney U test; for paired data, paired t-test and paired Wilcoxon signed-rank test were used. We used two-tailed statistical tests, where applicable. Effects in experiments involving several conditions were assessed using ANOVA. We used the Bonferroni procedure to adjust for multiple comparisons, unless otherwise stated. We applied Pearson's product-moment correlation to determine relationships between continuous variables. Pearson's χ^2 test was used to compare proportions between neural populations or experimental states. The χ^2 test for given probabilities was used to compare measured proportions against expected proportions. The significance threshold was set at 0.05. All data analysis was conducted using open source R packages, with the exception of MoSeq-related analysis, which was run in Python.